SCi
DEFENSE
DIVISION

(11) 15 September 1980

(12) B3

(9) Project No. 5302
Task 3 Technical Report: 27 Dec 78-15 Sep 80

LEVEL II

(6)

SIMULATION OF ADAPTIVE CLOSED-LOOP CONTROL PROCEDURES FOR ELECTRONIC COUNTERMEASURES.

(12) 104

Sponsored by:

DEFENSE ADVANCED RESEARCH PROJECTS AGENCY

(15)

ARPA Order No. 3613, Program Code No. 8G10
Monitored by NAVELEX under Contract No. N00039-79-C-0124, ARPA Order 3613
Period of Contract: 27 December 1978 to 15 September 1980
Reporting Period: 27 December 1978 to 15 September 1980

Approved by:

J.P. Marsh

J.P. Marsh
Manager,
Control Technology Program

Prepared by:

(10)

A. Joseph Rockmore
Paul L. Cowell
Scott Foster

DISTRIBUTION STATEMENT A
Approved for public release;
Distribution Unlimited

"The views and conclusions contained in this document are those of the authors and should not be interpreted as representing the official policies, either expressed or implied, of the Defense Advanced Research Projects Agency or the U.S. Government."

SYSTEMS CONTROL, INC. ■ 1801 PAGE MILL ROAD □ PALO ALTO, CA 94304 ■ TELEX 348-433 ■ (415) 494-1165

TABLE OF CONTENTS

TABLE OF CONTENTS (Cont'd)

1. INTRODUCTION

Techniques to accomplish the goals of electronic countermeasures (ECM) have been developed in the past by exploiting a specific feature of a system in a heuristic manner. In general, emphasis has been placed upon the development of a technique which has some effectiveness against a particular threat system, and the choosing of the parameters of the technique has received little attention. This report documents the results of the third task of the work Systems Control, Inc. (SCI) has performed to apply advanced concepts from modern estimation and control theories to provide improved performance of ECM systems. In this program, approaches to the design of techniques for ECM are developed, especially as related to the control, or time-varying choice of parameters of the technique, so as to achieve a specified performance objective.

Task I Technical Report [1] is concerned with the development of control procedures to vary the parameters of the ECM technique. These procedures are derived from the disciplines of control and estimation theories. They fall into the category of adaptive closed-loop jamming, where observables related to the radar (e.g., the time-varying power of a conical scan system, the actual threat antenna pointing angle, etc.) are used in a feedback structure to vary the control variables of an ECM technique (e.g., the amplitude of the pulses in a scan rate modulation ECM, the relative amplitude and phase of a cross-eye ECM, etc.). The unknown nature of the threat radar is what calls for adaptive controllers.

Task II Technical Report [2] is concerned with the application of the techniques described in [1] to three particular threat systems: conical scan on receive only (COSRO), pseudo-monopulse, and monopulse. Each threat system is analyzed in terms of available observables and an appropriate ECM technique. The connection between these two is provided by the adaptive controller, which takes the observable and feeds it back to the ECM control variable. The form of the controller takes on one of two forms, described

in [1]. The first is a parametric controller, which exploits the actual structure of the threat radar and controls using ideas from stochastic approximation. The second is an input/output controller, which assumes an auto-regressive moving average (ARMA) model relating the observables to the control variables, and does a model fit and control based on the model. Both of these approaches are employed against the specific systems of interest.

The current report is concerned with the simulation of the threat/target interaction to verify and explore aspects of the performance of the adaptive closed-loop approach to ECM. A scenario is postulated in which the threat, which is a ground-based or missile radar, illuminates a target, which is an aircraft or a ship. The emphasis in the current report has been on the problem of defending an aircraft against a ground-based threat, but elements of the antiship missile defense problem are included. The latter problem will receive more emphasis in the following phases of the project. Models used and results obtained are described.

This report assumes a fairly high degree of familiarity with the previous task technical reports. Thus details of the ECM techniques and derivation of the control procedures are omitted. Detail related specifically to the computer simulation are included, as well as results.

1.1 DESCRIPTION OF THE SIMULATION

The purpose of the simulation is to compare and evaluate the performance of various ECM systems designed to defeat one or more types of tracking radars. The simulated system is composed of two subsystems, the threat and the target. The threat system is a tracking radar which actively illuminates a target to establish its position. The target is the aircraft or ship being tracked and its ECM and ESM equipment.

A system, which may be defined as a collection of entities in a regular interaction, is modeled by a body of selected information which describe the salient system features to be studied. In general, the models are specified by the four structural elements described below.

(1) The entities: objects which comprise the system.

The system is composed of smaller subsystems and the corresponding entities may be grouped into a hierarchy of more general entities, such as:

- Threat
  - Airframe (if missile or aircraft) dynamics
  - Radar
    - Antenna
    - Servo motors
  - Tracking loop
    - Detector
    - Signal processing
    - Servo motor driver
- Target
  - Airframe (if aircraft) or ship dynamics
  - EW equipment
    - ESM antenna
    - Sensor processing
    - ECM controller
    - ECM technique generator
    - ECM antenna.

Each of the threat and target systems is composed of four basic subsystems:

- a sensor to detect radar energy
- a signal processor and controller
- a transmitter to generate radar energy
- a reflector of incident radar energy.

(2) The attributes: properties of the entities.

The attributes describe various properties of the entities, such as locations, pointing directions, antenna and filter parameters, and radar cross section.

(3) The activities: causes of change in the system.

The target and threat may be thought of as two separate but interacting systems which have a spatial, a temporal, and a physical relation. The two systems are spatially related in a coordinate system. Each may move so that the relation may be altered. The temporal relation is constrained to synchronous, pulse-by-pulse operation. The simulation is event-oriented in that it follows a history of activities which are applied to different entities.

This representation of the target-threat interaction leads to restrictions on the types of relationships that can be modeled. The timing in the current simulation is based on an interval-oriented clock that runs at the pulse repetition frequency (p.r.f.) of

the tracking radar. Because events occur only at the time of the simulation clock update, the threat and target run synchronously. This is not a necessary restriction on the simulation, but asynchronous operation has not yet been required in evaluating the ECM systems developed to date.

The physical relation is the transmission, reflection, and reception of radar energy by both systems. The basic activities which alter the entities are:

- Transmit a tracking pulse
- Transmit an ECM pulse
- Generate a skin return
- Detect the ECM and skin return
- Move the airframe or ship.

Some of these activities are deterministic, such as pulse transmission, while others are stochastic; the outputs are not completely specified in terms of the inputs. Clearly, these activities may be broken down even further into more fundamental activities which change the most basic entities in the system.

(4) The environment: changes which affect the system but occur outside of it.

The system-environment boundary includes the whole simulation; in other words, there are no exogenous activities, those that lie outside the system.

The simulation is structured as shown in Figure 1-1 to model a single engagement between a target airframe or ship moving on a pre-specified trajectory past a stationary, ground-based or moving threat. The threat motion can be in response to the radar return and ECM of the target, such as will be the case in a missile threat. An engagement is divided by the user into a number of segments by specifying the length of time which will elapse in each segment, where time is measured in pulses. Inputs to the simulation define the target and threat parameters, the target and threat trajectories, and control the simulation itself. Outputs include a complete list of all input parameters, aid to accurate numerical analysis or debugging, and graphical output showing temporal sequences or histograms. These outputs are under the control of a user who determines the number of pulses occurring at the threat radar p.r.f. in the next segment of the engagement and what output will be generated for it.

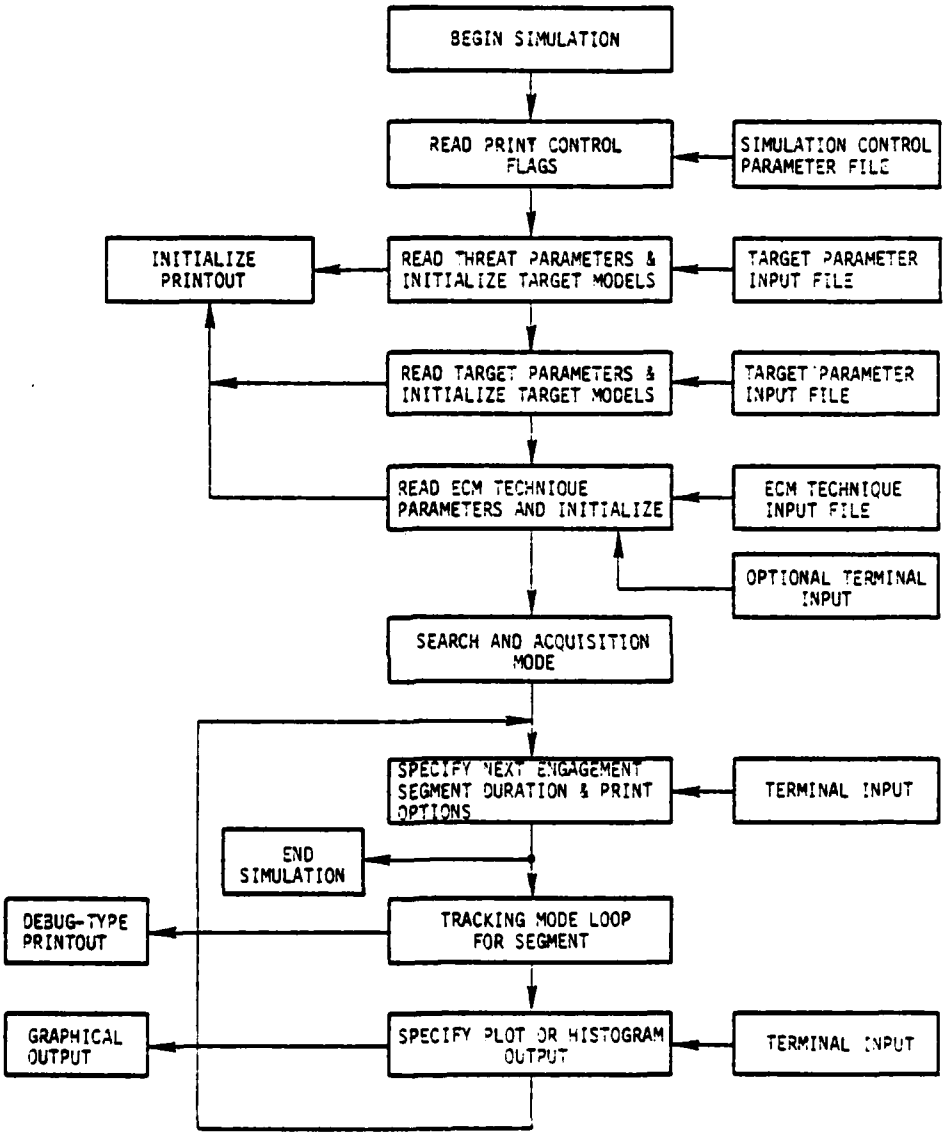

Figure 1-1. Structure of Simulation Program

The major part of the modeling of the threat, target, and ECM occurs in the tracking loop, shown in Figure 1-2. (The acquisition or search mode is essentially the same as the tracking mode except that no ECM is allowed and the antenna is forced to point near the target to allow the tracking loop to stabilize.) In the tracking loop, a pulse transmission from the threat radar illuminates the target. The resulting skin return, along with any ECM, are detected by the threat to provide an error signal which points the antenna through its servo motors. In order to accomodate a variety of threat antenna and signal processing components, a variety of target models, and a variety of ECM techniques, the tracking loop is broken into a set of interacting modules, as shown in Figure 1-3.

1.2 COORDINATE SYSTEMS

The physical relationships between the target and threat as they move with time must be referenced to a particular coordinate system. This coordinate system, described in Section 1.2.1, is a topocentric-horizon coordinate system called the SEZ system, for South-East-Z axis. It is thus a Cartesian coordinate system.

The antenna gain patterns for all antennas must be referenced to a translated Cartesian coordinate system, denoted the S'E'Z' system. This system is described in Section 1.2.2.

Since the target may be an extended target (as in the ship case) or its ECM technique may depend on spatially separated emitters (as in the cross-eye case), a separate coordinate system must be defined for the target. This system, described in Section 1.2.3, is called the RPY system, for Roll axis-Pitch axis-Yaw axis. It is thus also a Cartesian coordinate system.

1.2.1 Topocentric-Horizon (SEZ) Coordinates

The threat and the target are located in a common coordinate system fixed on the surface of the earth called the topocentric-horizon system, shown in Figure 1-4.

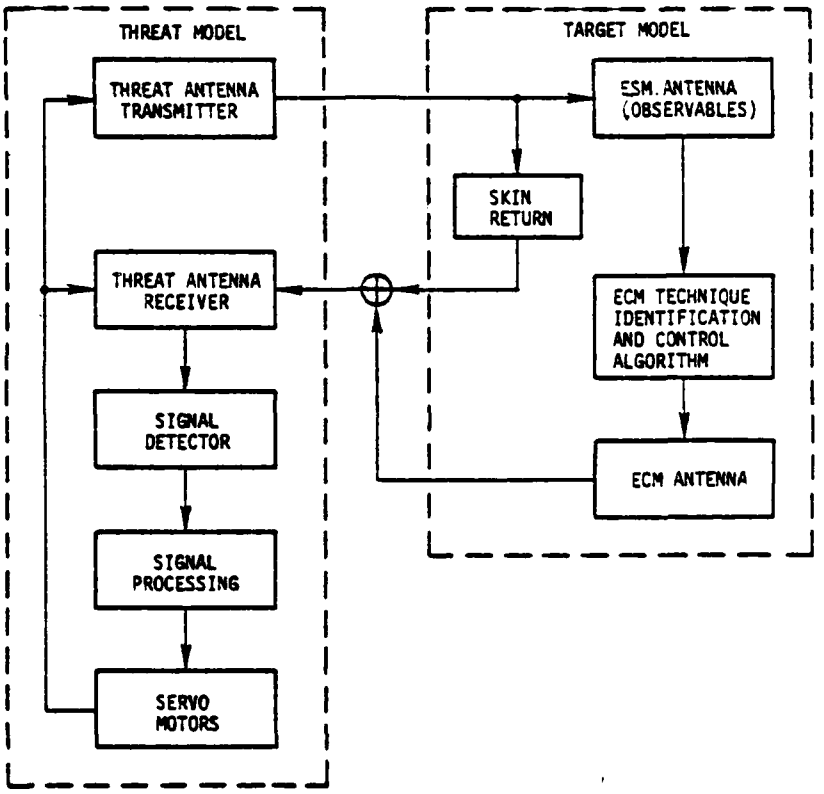

Figure 1-2. Tracking Loop Diagram

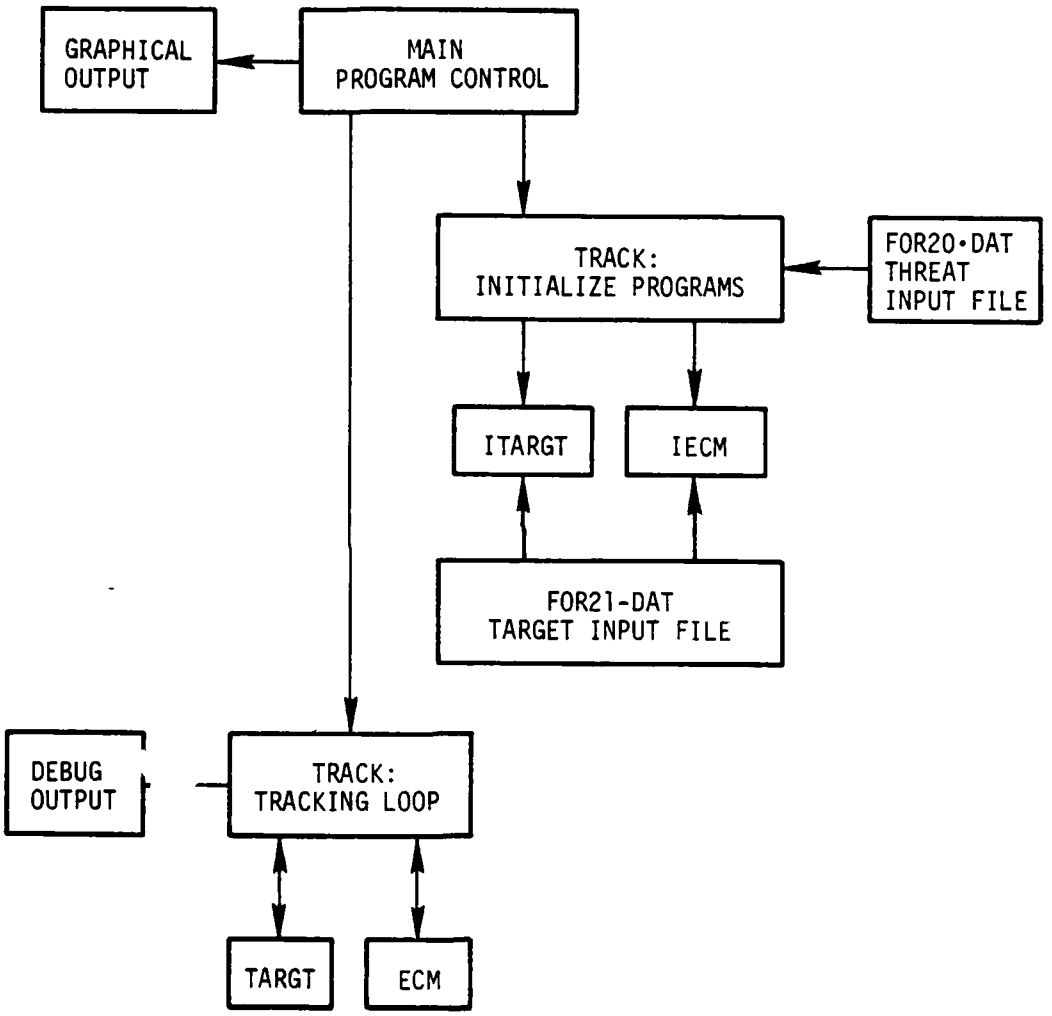

Figure 1-3. Modular Structure of Simulation

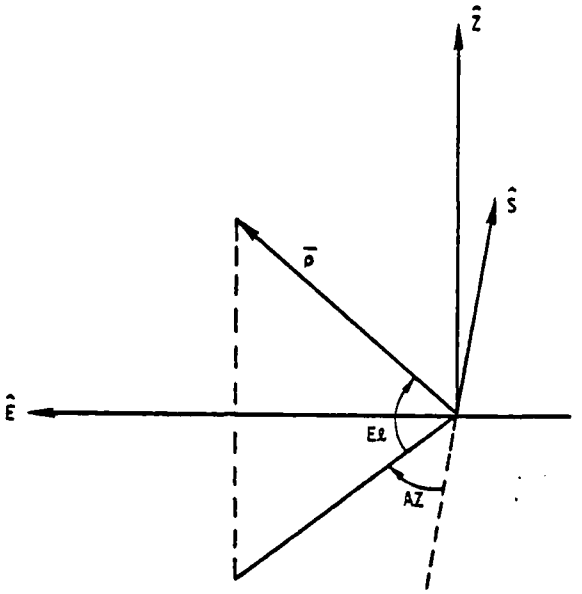

Figure 1-4. Topocentric-Horizon Coordinate System

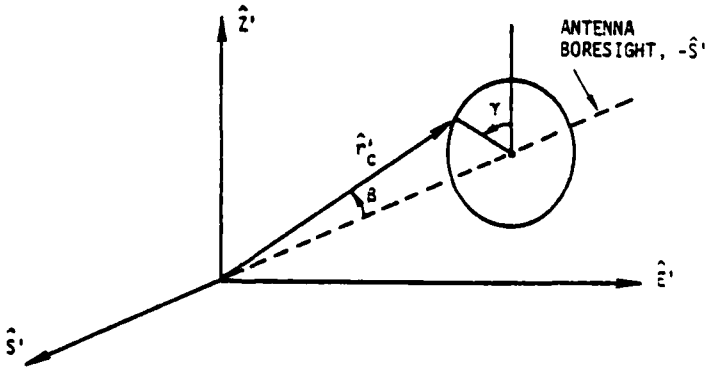

Figure 1-5. Angles Shown for Antenna Pointing Due North

The origin is located at the position of the fixed, ground-based radar associated with the threat, or at an arbitrary place if there is no fixed threat radar. The S-E plane coincides with the horizon plane, with S pointing south and E pointing east. The Z-axis points toward the Zenith. Any vector $\bar{\rho}$ may be expressed in these coordinates by

$$\bar{\rho} = \rho_S S + \rho_E E + \rho_Z Z \ .$$

The azimuth and elevation angles and the magnitude of the vector are defined by

$$AZ = \arctan \rho_E/(-\rho_S)$$

$$E\ell = \arcsin \rho_Z/\rho$$

$$\rho = (\rho_S^2 + \rho_E^2 + \rho_Z^2)^{1/2} \ .$$

The inverse transformation is given by:

$$\rho_S = -\rho \cos E\ell \cos AZ$$

$$\rho_E = \rho \cos E\ell \sin AZ$$

$$\rho_Z = \rho \sin E\ell \ .$$

1.2.2 Antenna Coordinate System and Beam Geometry

In general, an antenna gain pattern associated with the antenna will not necessarily be aligned with the antenna axis. A coordinate system attached to the antenna to describe the orientation of its gain pattern is shown in Figure 1-5. It has translated coordinates S'E'Z', corresponding to translated South, translated East, and translated Zenith. The coordinate system axes coincide with the topocentric-horizon system axes when the antenna is pointed due north (zero azimuth and zero elevation). The gain pattern location is described by its squint angle, β, and phase angle, γ.

The SEZ coordinate system may be transformed by two successive rotations into the S'E'Z' coordinate system, as shown in Figure 1-6. The first rotation is made about the $\hat{Z}$-axis through angle AZ, the azimuth angle. The second is made about the new $\hat{E}$-axis through $E\ell$, the elevation angle. Denote an arbitrary vector by

$$\rho = \rho_S \hat{S} + \rho_E \hat{E} + \rho_Z \hat{Z} = \rho'_S S' + \rho'_E E' + \rho'_Z Z' \ .$$

Then the coordinate transformation may be written

$$\begin{pmatrix} \rho'_S \\ \rho'_E \\ \rho'_Z \end{pmatrix} = R_y(-E)\ R_z(-A) \begin{pmatrix} \rho_S \\ \rho_E \\ \rho_Z \end{pmatrix}$$

$$= \begin{pmatrix} \cos E & 0 & -\sin E \\ 0 & 1 & 0 \\ +\sin E & 0 & \cos E \end{pmatrix} \begin{pmatrix} \cos A & -\sin A & 0 \\ \sin A & \cos A & 0 \\ 0 & 0 & 1 \end{pmatrix} \begin{pmatrix} \rho_S \\ \rho_E \\ \rho_Z \end{pmatrix} .$$

When the antenna axis is pointed at (A_o, E_o), the vector $\hat{r}'_c$ along the gain pattern axis can be expressed in the topocentric-horizon system by

$$\hat{r}_c = R_z(+A_o)\ R_y(+E_o)\ \hat{r}'_c \ .$$

The simulation is capable of modeling antennas with multiple beams whose locations are defined relative to the boresight of the antenna in the antenna coordinate system.

Figure 1-7 shows the parameters used to define the beams, each of which is squinted relative to the antenna boresight by an angle β^j and is located at a true phase angle γ_o^j from the elevation axis. Table 1-1 indicates the names of the quantities used in the simulation.

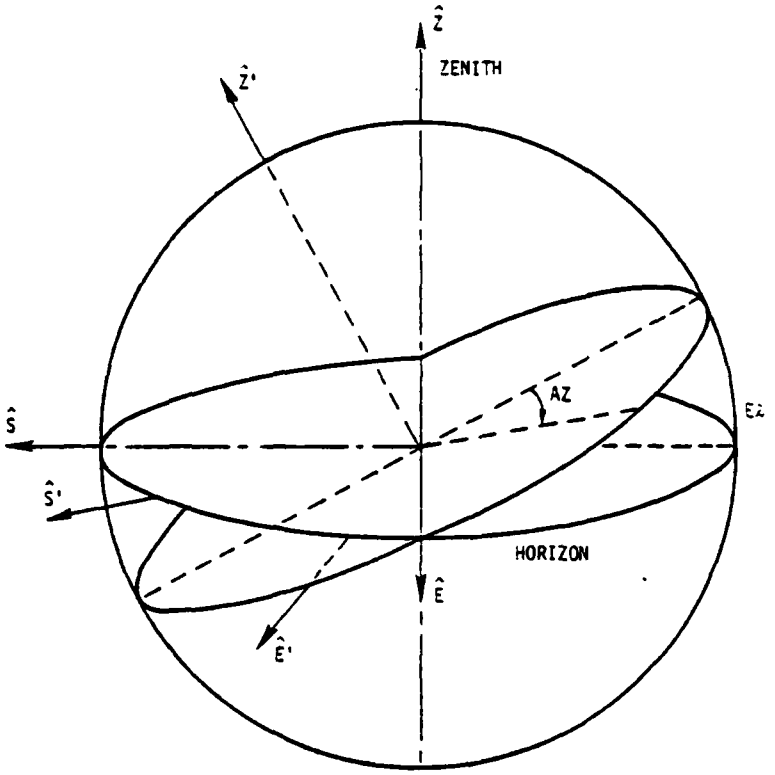

Figure 1-6. Relationship Between Topocentric-Horizon (SEZ) and Antenna-Based ($S'E'Z'$) Coordinate Systems

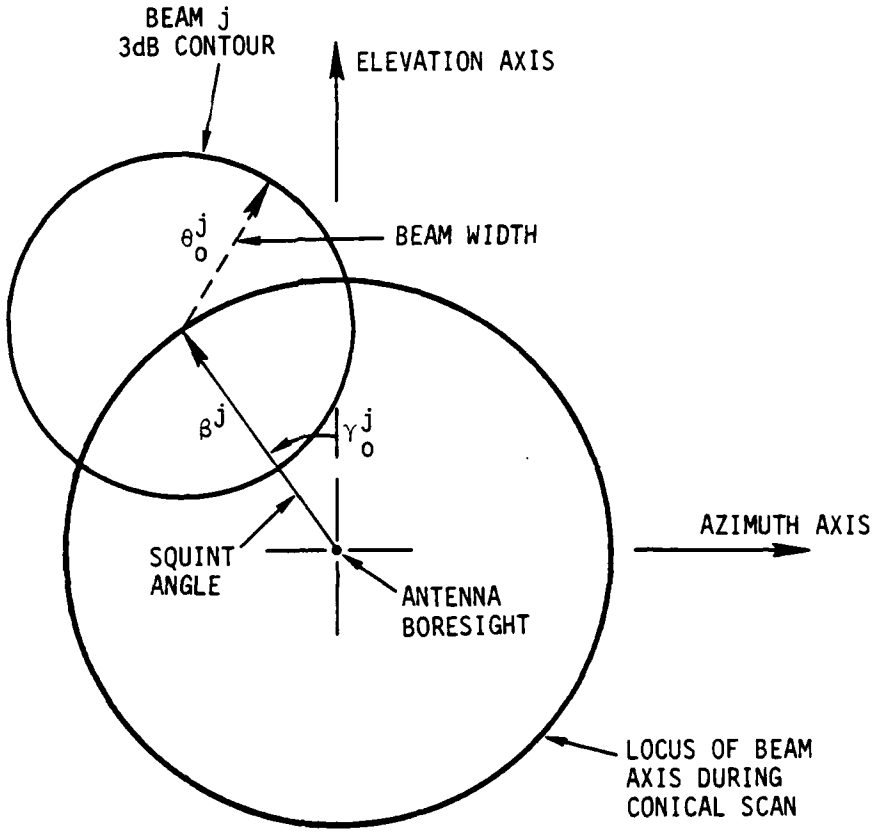

Figure 1-7. Multiple Beam Geometry

Table 1-1. Beam Geometry Description Input to Program IANTG

SYMBOL	VARIABLE NAME	DESCRIPTION
N	NB	Number of beams
β^j	BETA	Squint angle of beam
γ_o^j	GAMMA	Initial phase angle of beam
$G_j(0)$	GNAXIS	Beam gain (if transmitter)
θ_o^j	BWDEG	3 dB (half) beamwidth in degrees
A^j	RCVARE	Beam effective aperture in m^2 (if receiver)

When the phase angle of any beam, γ^j, depends on time, the antenna system is described as a conical scanning system.

Antennas with conical scanning beams are modeled by computing new beam positions in the antenna coordinate system on every pulse.

The inputs required for conical scanning antenna system are shown in Table 1-2. For each pulse, the phase of each beam is updated in the program CSG, if the beam is rotated by a conical scan mechanism according to

$$\gamma_k = (\gamma_{k-1} + d\gamma) \bmod(2\pi) \ .$$

A unit vector, r_k', along each beam axis in the antenna coordinate system is computed from

$$r_k' = (-\cos \beta^j, -\sin \beta^j \sin \gamma_k, +\sin \beta^j \cos \gamma_k)^T \ .$$

Table 1-2. Conical Scanning Antenna Parameters in Program ICSG

SYMBOL	VARIABLE NAME	DESCRIPTION
f_r	PRFREQ	Pulse repetition frequency
f_c	CSFREQ	Conical scan frequency
ϕ_c	CSPHAS	Reference signal phase shift
$d\gamma$	DELGAM	Conical scan phase increment per pulse $= 2\pi f_c f_r^{-1}$

All of the beams rotate together in a conical scan system about the antenna boresight, maintaining their relative phase angles constant. The reference signals are computed relative to the position of the first beam by

$$A_k^{ref} = -\sin(\gamma_k + \phi_c)$$

$$E_k^{ref} = +\cos(\gamma_k + \phi_c) \ .$$

In the tracking radar, the servo motors drive the antenna in a direction based on the error signal derived from the radar returns. Those corrections, dA_k and dE_k obtained from the servo motor models, are applied to the current antenna position and the true position of the target within the antenna beams is obtained.

The servo output updates the antenna pointing angles:

$$A_k = A_{k-1} + dA_k \, f_r^{-1}$$

$$E_k = E_{k-1} + dE_k \, f_r^{-1} \ .$$

The current antenna boresight axis is then defined by

$$b_k = (-\cos E_k \cos A_k, +\cos E_k \sin A_k, \sin E_k)^T .$$

Denoting by ρ_k the vector from the threat to the true target position, the true azimuth and elevation of the target are given by

$$\tan A_k^o = -\rho_k \cdot \hat{E} (\rho_k \cdot \hat{S})^{-1}$$

$$\sin E_k^o = \rho_k \cdot \hat{Z} \, |\rho_k|^{-1} .$$

The beam axes are rotated into the SEZ coordinate system by the successive rotations

$$r_k = \begin{pmatrix} \cos A_k^o & \sin A_k^o & 0 \\ -\sin A_k^o & \cos A_k^o & 0 \\ 0 & 0 & 1 \end{pmatrix} \begin{pmatrix} \cos E_k^o & 0 & \sin E_k^o \\ 0 & 1 & 0 \\ -\sin E_k^o & 0 & \cos E_k^o \end{pmatrix} r_k' .$$

The angle of the line-of-sight to the target from each beam axis is then given by

$$\cos \alpha_k = \rho_k \cdot r_k \, |\rho_k|^{-1} .$$

These calculations are performed in program AUTGEO, whose variables are described in Table 1-3.

The antenna beam patterns all follow a $(\sin x/x)^2$ shape with the beamwidth as a parameter. The one-way antenna gain relative to its maximum value is given by

$$g(\theta) = \begin{cases} 1 - x^2/6 & x \leq 0.03 \\ (x^{-1} \sin x)^2 , & x > 0.03 \end{cases}$$

Table 1-3. Variables in Program AUTGEO

SYMBOL	VARIABLE NAME	DESCRIPTION
A_k	ANTAZ	Antenna boresight azimuth
E_k	ANTEL	Antenna boresight elevation
b_k	BORE	Unit vector along antenna boresight axis
ρ_k	RHO	Vector from threat to target
$\lvert\rho_k\rvert$	RANGE	Range to target
A_k^o	AZTRUE	True target azimuth
E_k^o	ELTRUE	True target elevation
r_k'	RBMV	Unit vector along beam axis, S'E'Z' system
r_k	ABMV	Unit vector along beam axis, SEZ system
α_k	THETA	Angle of target off beam axis

where $x = 1.4\ \theta/\theta_o$ and the beamwidth is $2\theta_o$. When $\theta = \theta_o$, the antenna gain is 3 dB down from its value at $\theta = 0$ or $g(\theta) = 0.5$. Thus to have a 2° beamwidth, $\theta_o = 1°$ is chosen.

1.2.3 Target (RPY) Coordinate System and Target Geometry

A coordinate system attached to the target has been defined to specify the locations of scatterers and emitters attached to the airframe or ship. An aspect-dependent cross-section model may also be specified in this system.

The target coordinate system has its origin at the center of gravity (CG) of the airframe with the roll axis, $\hat{R}$, in the aft direction, the pitch axis, $\hat{P}$, toward the right side, and the yaw axis, $\hat{Y}$, vertical when the target is level relative to the surface.

The location of any point in the target system, ρ_{RPY}, is related to its location in the SEZ system by a translation and a rotation:

$$\rho_{SEZ} = \rho_S\hat{S} + \rho_E\hat{E} + \rho_Z\hat{Z}$$

$$= \rho_{CG} + \rho_R\hat{R} + \rho_P\hat{P} + \rho_Y\hat{Y} ,$$

where ρ_{CG} is the location of the target CG in the SEZ system.

The rotation matrix, $M(\theta_Y, \theta_P, \theta_R)$ of the coordinates ρ_{RPY} in the RPY system to coordinates ρ'_{SEZ} in the SEZ system with origin at the target CG is

$$\begin{pmatrix} \rho'_S \\ \rho'_E \\ \rho'_Z \end{pmatrix} = \begin{pmatrix} +\cos\theta_Y & +\sin\theta_Y & 0 \\ -\sin\theta_Y & +\cos\theta_Y & 0 \\ 0 & 0 & 1 \end{pmatrix} \begin{pmatrix} +\cos\theta_P & 0 & +\sin\theta_P \\ 0 & 1 & 0 \\ -\sin\theta_P & 0 & +\cos\theta_P \end{pmatrix}$$

$$\cdot \begin{pmatrix} 1 & 0 & 0 \\ 0 & \cos\theta_R & -\sin\theta_R \\ 0 & \sin\theta_R & \cos\theta_R \end{pmatrix} \begin{pmatrix} \rho_R \\ \rho_P \\ \rho_Y \end{pmatrix} .$$

The translation is simply $\rho_{SEZ} = \rho_{CG} + \rho'_{SEZ}$.

The angles θ_R, θ_P, and θ_Y are the roll, pitch, and yaw of the target in the SEZ system. The velocity, $\bar{v}$, of the target is aligned with the $-\hat{R}$ axis and has the coordinates

$$\bar{v} = |\bar{v}|(-\cos\theta_Y \cos\theta_P, +\sin\theta_Y \cos\theta_P, \sin\theta_P)^T .$$

The velocity vector determines the orientation of the target coordinate system except for the roll angle:

$$\sin\theta_P = \bar{v} \cdot \hat{Z} \; |\bar{v}|^{-1}$$

$$\tan\theta_Y = \bar{v} \cdot \hat{E}(-\bar{v} \cdot \hat{S})^{-1}$$

$$\theta_R = 0 .$$

The positive sense of rotation for these angles is

Roll — right side up,
Pitch — forward end up,
Yaw — right turn.

Thus, the location r_k' of any emitter or reflector in the target at time k is given in the SEZ system by

$$r_k' = \rho_{CG} + M(\theta_R, \theta_P, \theta_Y) r_k \ .$$

A further rotation is used to align the antenna boresight axis with North $(-\hat{S})$:

$$r_k'' = \begin{pmatrix} \cos E_o & 0 & -\sin E_o \\ 0 & 1 & 0 \\ \sin E_o & 0 & \cos E_o \end{pmatrix} \begin{pmatrix} \cos A_o & -\sin A_o & 0 \\ \sin A_o & \cos A_o & 0 \\ 0 & 0 & 1 \end{pmatrix} r_k' \ .$$

The angles A_o and E_o are the azimuth and elevation angles of the antenna boresight axis. The angles of the source at r_k projected on the azimuth and elevation axes are then easily found from

$$\tan \theta_k^{AZ} = (r_k'' \cdot \hat{E})(-r_k'' \cdot \hat{S})^{-1}$$

$$\sin \theta_k^{EL} = (r_k'' \cdot \hat{Z}) \ |r_k''|^{-1} \ .$$

The range difference from the source to the CG along the line-of-sight from the antenna is

$$\Delta = (r_k' - \rho_{CG}) \cdot \rho_{CG} \ |\rho_{CG}|^{-1} \ .$$

1.3 RADAR SIGNAL PROCESSING

The digital signal processing required by tracking radars employing pulsed waveforms is described in this section. These filters are used in removing noise, detecting the amplitude modulation at the conical scan frequency, and modeling the servo motors which point the antenna. The specific descriptions of the threat models and ECM controllers of Sections 3 through 5 should be consulted to find how specific filters are used within a model and what their parameter values are.

1.3.1 Digital Filters

Most digital filters have been developed from transfer functions written for analog filters in the continuous frequency domain where they are described by their gain and the locations of their poles and zeroes. The transfer function for the analog filter, $H_a(S)$, is transformed into the corresponding discrete filter by means of the backward difference operator, where T is the sample interval:

$$TS = 1 - Z^{-1} .$$

In the same way that the transfer function represents a differential equation, the resulting system function, $H(Z)$, represents a difference equation which can be retrieved to provide the time-domain representation of the filter [3]. Table 1-4 lists some of the filters used in the simulation and the method of generating the output sequence, y_k, from the input sequence, x_k.

The analog transfer function has the form

$$H_a(S) = \frac{(2\omega_o/Q)(S + S_o)}{S^2 + (2\omega_o/Q)S + \omega_o^2} ,$$

where $Q = f_o(2\Delta f)^{-1}$ and $f_o = \omega_o(2\pi)^{-1}$ is the resonant frqeuency and Δf the bandwidth of the filter.

The same transfer function represented by poles and zeroes is

$$H_a(S) = K(1 + S/a)(1 + S/b)^{-1}(1 + S/c)^{-1} ,$$

where

$$b,c = \omega_o[Q^{-1} \pm (Q^{-2} - 1)^{1/2}]$$

$$a = S_o$$

$$K = 2S_o(\omega_o Q)^{-1} .$$

Table 1-4. Digital Filters

PROGRAM	ANALOG	DIFFERENCE EQUATION
POLEA (ILPF1,LPF1) (ILPF2,LPF2) (ILPF3,LPF3	$G(1+S/a)^{-1}$	$(1+aT)y_k = y_{k-1}+G(aT)x_k$
POLEAA	$G(1+S/G)^{-2}$	$(1+aT)^2 y_k = G(aT)^2 x_k+2(1+aT)y_{k-1} - y_{k-2}$
FILZP	$G(1+S/a)(1+S/b)^{-1}$	$(aT)(1+bT)y_k = G(bT)[(1+aT)x_k -x_{k-1}]+(aT)y_{k-1}$
FILZPP	$\frac{G(1+S/a)}{(1+S/b)(1+S/c)}$	$(aT)(1+CT)(1+bT)y_k = (aT)(2+bT+cT)y_{k-1} -(aT)y_{k-2}+G(bT)(cT)[(1+aT)x_k-x_{k-1}]$
BPFZPP	$\frac{2(a/Q)G(S+b)}{s^2+2Sa/Q+a^2}$	$[1+(2aT/Q)+(aT)^2]y_k = 2(1+aT/Q)y_{k-1} +y_{k-2}+2G(aT/Q)[(1+bT)x_k-x_{k-1}]$

Given the locations of the poles, b and c, and the zero, a, the inverse transformation is

$$\omega_o^2 = bc$$

$$S_o = a$$

$$2\omega_o Q^{-1} = b + c = Kbca^{-1} .$$

The gain is not an independent parameter, so that the transfer function becomes, upon replacing K;

$$H_c(S) = (b+c)(S+a)(S+b)^{-1}(S+c)^{-1} .$$

The discrete-time version of the filter is shown in Table 1-4.

1.3.2 Automatic Gain Control

The AGC is a nonlinear device which uses a linear filter to produce its output. The input sequence, z_k, is averaged by a linear low-pass filter to produce the average signal z'_k. The input sequence is passed through a variable gain equal to z'^{-1}_k. To produce the AGC output, $z''_k = z_k/z'_k$, as shown in Figure 1-8.

Programs IAGCH and AGC4 implement an AGC model employing a low-pass filter with one pole.

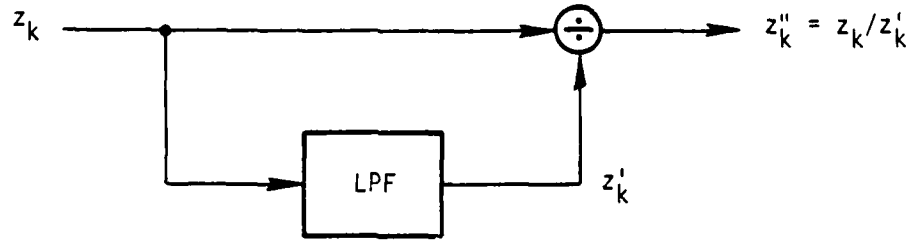

Figure 1-8. AGC Block Diagram

1.3.3 Antenna Servomechanism Models

The transfer function for the input error voltage, v, and the output shaft rotation angle, δ, is assumed to be of the form:

$$\delta/v = K(1+S/\omega_1)^{-1}(1+S/\omega_3) \ .$$

The corresponding z-transform obtained from the replacement $TS = 1-z^{-1}$ is

$$H(z) = K[1+(1-z^{-1})/(T\omega_1)]^{-1}[1+(1-z^{-1})/(T\omega_3)] \ ,$$

which corresponds to a difference equation for computing the output sequence, δ_k, given by

$$(T\omega_3)(1+T\omega_1)\delta_k = K(T\omega_1)[(1+T\omega_3)v_k - v_{k-1}] + (T\omega_3)\delta_{k-1} \ .$$

The shaft rotations are integrated by a filter with the transfer function

$$A(S)/\delta(S) = S^{-1} \ ,$$

whose z-transform is

$$H(z) = T(1-z^{-1})^{-1} \ .$$

The difference equation is thus:

$$A_k = A_{k-1} + T^{-1}\delta_k \ .$$

Programs ISERV2 and SERVO2 implement this model.

A second approach to implementing the servos is to use a bilinear transform. The servo motor transfer function is used together with the bilinear transform:

$$TS = 2(1-z^{-1})(1+z^{-1})^{-1} \ .$$

to obtain the corresponding z-transform:

$$H(z) = K \frac{z^{-1}(1 - 2/T\omega_3) + (1 + 2/T\omega_3)}{z^{-1}(1 - 2/T\omega_1) + (1 + 2/T\omega_1)} = \frac{\delta(z)}{v(z)} .$$

The resulting difference equation for the output sequence δ_k is

$$(1 + 2/T\omega_1)\delta_k + (1 - 2/T\omega_1)\delta_{k-1} = K[(1 + 2/T\omega_3)v_k + (1 - 2/T\omega_3)v_{k-1}] .$$

Program ISERV3 is used to initialize program SERVO2 when this servo model is desired.

1.3.4 Error Detector in Conical Scan System

In a conical scan radar, the error information is encoded in the amplitude and phase of the modulation of the detected signal at the conical scan frequency. This information is extracted as a vector error, $(\alpha_k, \varepsilon_k)$.

The phase of the conical system is defined by

$$(A_k^{ref}, E_k^{ref}) = [-\sin(\gamma_k + \phi), \cos(\gamma_k + \phi)] ,$$

where $\gamma_k = 2\pi f_c f_r k$ is the true phase angle of the conical scanning beam, ϕ is a phase shift to account for the phase delay in the error signal as it is processed by various filters, f_c is the conical scan frequency, and f_r is the pulse repetition frequency.

The error signals for each component of the angle error are then obtained from the error signal, V_k'', by:

$$\alpha_k = \frac{V_g}{\ell} \sum_{j=k}^{k+\ell-1} V_j'' A_j^{ref}$$

$$\varepsilon_k = \frac{V_g}{\ell} \sum_{j=k}^{k+\ell-1} V_j'' E_j^{ref} ,$$

where ℓ is the number of pulses over which the error is computed.

Programs IAEDET and AEDET represent this model.

1.4 THE SCENARIO

The modules related to the scenario to be exercised are described in this section. The target models are given in Section 1.4.1. These include the model of radar cross-section, the ECM antenna model, and the ESM antenna model. Section 1.4.2 describes the trajectories of the target and threat. For the current phase of the project, the threat is stationary. Thus only the target trajectory is given. The ECM objective is described in Section 1.4.3. This objective is the desired angle error as a function of time which the ECM system is attempting to induce in the threat radars.

The models describing the threat portion of the scenario are relegated to the sections describing each radar type: conical scan systems in Section 2, psuedo-monopulse systems in Section 3, and monopulse systems in Section 4. This is because each threat model is specific to the system, with relatively little commonality.

1.4.1 Target Model

The target model includes the following aspects related to the target platform:

- Radar cross-section
- ESM antenna
- ECM antenna.

Each of these models is described in detail below. The target programs provide an interface between the tracking radar and the programs which model the ECM techniques.

In this phase of simulation development, the weapon employed by the threat has been simplified to anti-aircraft artillery (AAA) with no pointing angle errors of its own. However, the simulation is capable of incorporating either active or semi-active homing or command-guided missile weapons. These will be addressed in the next phase of the project.

Radar Cross-Section Model

The target radar cross-section can be chosen from one of three available fluctuation models: deterministic, exponential, or Rayleigh. The correlation time of the fluctuations can also be controlled. The symbols in the program RCSGEN are described in Table 1-5.

The distribution of cross-section, σ_2, when the exponential model is used, is given by:

$$f(\sigma_2) = \bar{\sigma}_2^{-1} \; e^{-\sigma_2/\bar{\sigma}_2} , \qquad \sigma_2 \geq 0 .$$

This distribution for σ_2 is generated by selecting a pseudo-random number, r, distributed uniformly

$$f(r) = 1 , \qquad 0 \leq r \leq 1 ,$$

and then making the transformation $\sigma_2 = -\bar{\sigma}_2 \; \ell nr$. It has the average value $\bar{\sigma}_2$.

The distribution of cross-section, σ_4, when the Rayleigh distribution is selected, is given by:

$$f(\sigma_4) = 4\sigma_4 \; \bar{\sigma}_4^{-2} \; e^{-2\sigma_4/\bar{\sigma}_4} , \qquad \sigma_4 \geq 0 .$$

It has the mean $\bar{\sigma}_4$ and cumulative distribution:

$$F(x) \equiv \int_0^x \sigma_4 \; f(\sigma_4) d\sigma_4 = 1 - (1 + 2x/\bar{\sigma}_4) \; e^{-2x/\bar{\sigma}_4} .$$

The distribution for σ_4 is generated by selecting a pseudo-random number, r, distributed uniformly on [0,1] and solving the equation $F(x) = r$ for x. This is done iteratively using Newton's method in the program RAYLGH.

Table 1-5. Variables in Radar Cross-Section Model, IRCSGN and RCSGEN

SYMBOL	VARIABLE NAME	VALUE	DESCRIPTION
σ_o	RCSDET	0.0	Deterministic cross-section, m^2
$\bar{\sigma}_1$	RCS2	0.0	Average exponential cross-section, m^2
$\bar{\sigma}_4$	RCS4	10.0	Average Rayleigh cross-section, m^2
τ	RCSTIM	0.02	Correlation time of cross-section, sec.
f_r	PRFREQ	400.0	Pulse repetition frequency
σ_2			Cross-section from exponential distribution
σ_4			Cross-section from Rayleigh distribution
σ'_k			Uncorrelated cross-section at pulse k
σ_k			Correlated cross-section at pulse k
α_τ	RCSMKV		Correlation time filter parameter

The uncorrelated cross-section at pulse k, σ'_k, is then formed from the sum

$$\sigma'_k = \sigma_0 + \sigma_2 + \sigma_4 \ .$$

The cross-section is correlated using a first-order auto-regressive (Markov) filter defined by

$$\sigma_k = \alpha \ \sigma_{k-1} + (1 - \alpha) \ \sigma'_k \ .$$

The expected value of the correlated sequence is unchanged. The variance of correlated sequence is given by:

$$\text{var}[\sigma_k] = (1 - \alpha)(1 + \alpha)^{-1} \ \text{var}[\sigma'_k] \ .$$

The auto-covariance function of the output sequence at lag k is given by:

$$\gamma_k = \text{cov}[\sigma_n, \ \sigma_{n+k}] = \alpha \ \gamma_{k-1} \ .$$

A recursion relation for the auto-correlation function, defined by $\rho_k = \gamma_k / \gamma_o$, is then obtained as:

$$\rho_k = \alpha \ \rho_{k-1} \ , \qquad \rho_o = 1 \ ,$$

whose solution is

$$\rho_k = \alpha^k \ , \qquad k \geq 0 \ .$$

The correlation time of the sequence, τ , is defined from its auto-correlation function by

$$\rho_k = \alpha^k = e^{-t/\tau} \ ,$$

where the time at sample k is given by $t = kf_r^{-1}$. Thus, the parameter α is related to correlation time by

$$\alpha = e^{-(\tau f_r)^{-1}} .$$

The monopulse target model allows multiple point sources of radar energy which can be either reflectors or ECM emitters. The jth source is located in the airframe RPY coordinate system by the vector $r(j)$. The cross-section model for each scatter is identical to that for point sources, except that its phase may be specified to be either fixed or chosen uniformly between 0 and 2π. For those sources which are ECM emitters, the amplitude and phase is determined by the ECM control algorithm.

The ECM Antenna Model

The ECM antenna model interfaces the ECM technique controller to the tracking radar model by computing the emitted power in appropriate units and allowing some flexibility through appropriate input parameters.

The directed ECM power per pulse, P_k^{ECM}, emitted by the ECM antenna is given by

$$P_k^{ECM} = P^{ECM} \cdot G_k^{ECM} \cdot u_k ,$$

where: P^{ECM} = ECM antenna power in watts,

G_k^{ECM} = ECM antenna gain,

u_k = ECM control signal.

The current model for G_k^{ECM} is a constant, modeling an antenna always pointed at the threat.

ESM Antenna Model

The ESM model includes a very specific model for the power per pulse illuminating the target, and may also refer, in general, to any other observables which are used by specific ECM techniques. Only the model for a passive antenna is described here.

Given that power density p_k is incident on the ESM antenna at pulse k, the observable produced by the antenna is the power received:

$$P_k^{ESM} = G_k^{ESM} \cdot A^{ESM} \cdot P_k ,$$

where A^{ESM} is the effective antenna aperture and G_k^{ESM} is the relative gain of the antenna. For the current phase, it is the same as the relative gain of the ECM antenna,

$$G_k^{ESM} = G_k^{ECM} ,$$

modeling ganged antennas.

Specific ECM techniques should be consulted for a description of any other observables used.

1.4.2 Target Trajectory

The current interface is sufficiently flexible that any trajectory could be flown. On every pulse, an entry to the trajectory generator is made to compute the location and orientation of the target. The orientation is used as input to a more detailed cross-section model only for the monopulse threat.

The current trajectory generator allows a straight-line path defined by an initial position and velocity. At each pulse, k, a new position is computed from

$$r_k = r_{k-1} + f_r^{-1} v_o \ .$$

The standard trajectory is shown in Figure 1-9.

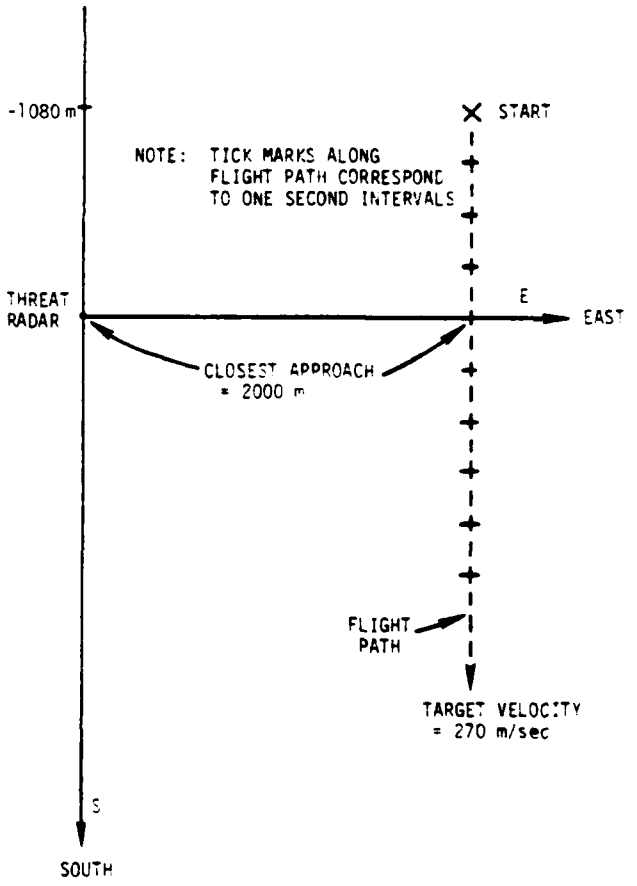

Figure 1-9. Engagement Scenario

2. CONICAL SCAN SYSTEMS

In a conical scanning radar, there are one or more beams which are either mechanically or electrically rotated about the boresight of the antenna. The beam rotation causes the received signal to be modulated at the rotation frequency with a depth of modulation which grows with an increase in the angle between the target and the antenna boresight and a phase related to the direction of the target off boresight. The resulting amplitude-modulated signal is processed to retrieve the depth of modulation and phase as input to the servo motors which move the antenna boresight toward the target. A variant of the basic conical scan radar is conical scan on receive-only (COSRO), where the transmit beam is fixed at the antenna boresight and the receiving beam performs the scanning. This is the basic system considered herein.

This section describes the conical scanning threat model and several ECM techniques which have been developed to deny tracking to the threat.

2.1 CONICAL SCAN THREAT TRACKING LOOP

The block diagram of the simulation for the conical scanning threat model is shown in Figure 2-1. The major signal processing functions are shown along with the interface between the threat and target models.

The beam geometry requires that two beams be defined, one for transmission and one for reception. Figure 2-2 shows the beams for a CONSCAN system where both beams coincide. Figure 2-3 shows the beam geometry for a COSRO system. The latter will be emphasized in this section.

The transmitting beam gain in the direction of the target is denoted by $G^T(\alpha_k^T)$. The power density illuminating the target is then

$$p_k = P^T G^T(\alpha_k^T)(4\pi |\rho_k|^2)^{-1} , \qquad (2.1)$$

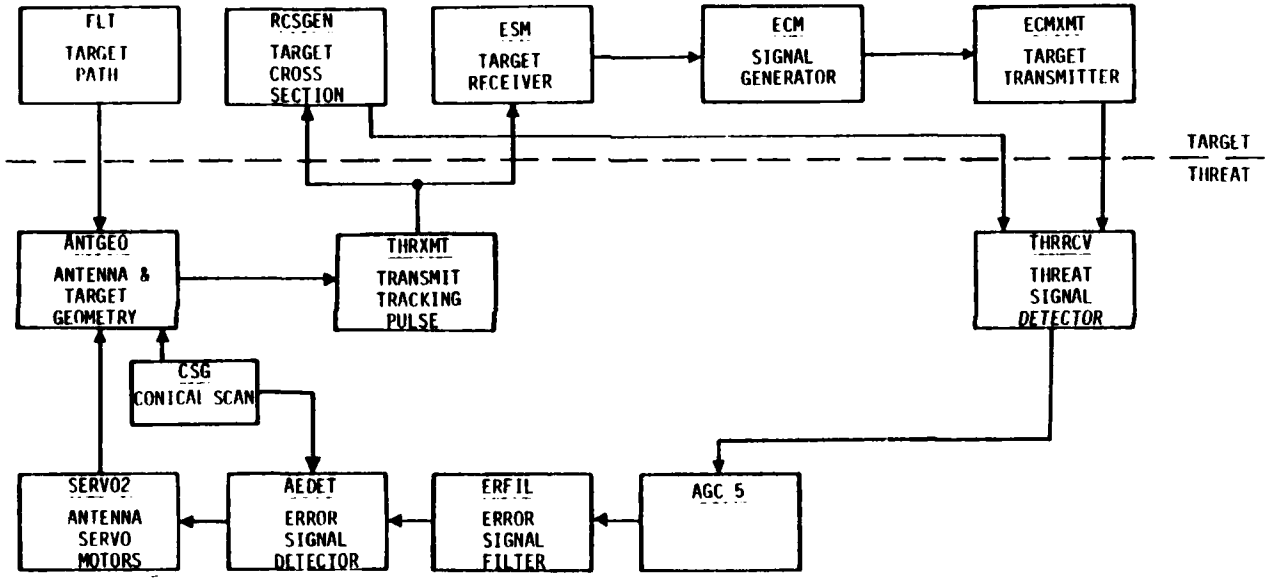

Figure 2-1. Conical Scan Threat Model Block Diagram Showing Program Names

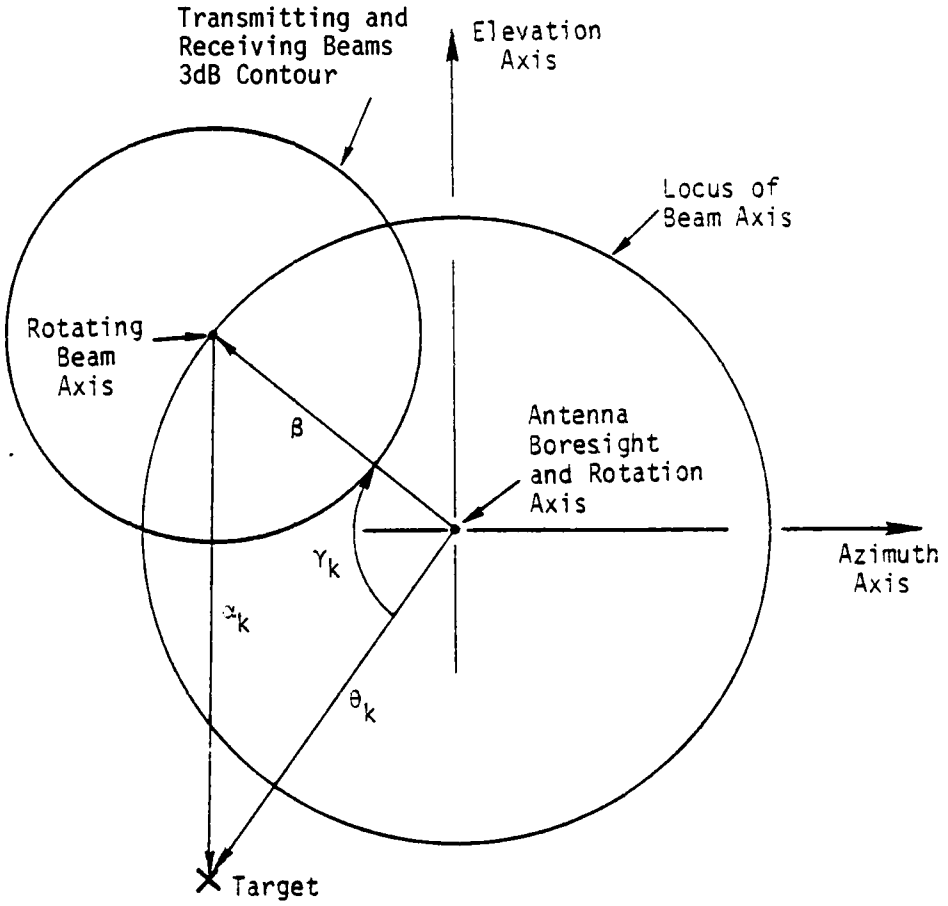

Figure 2-2. CONSCAN Beam Geometry

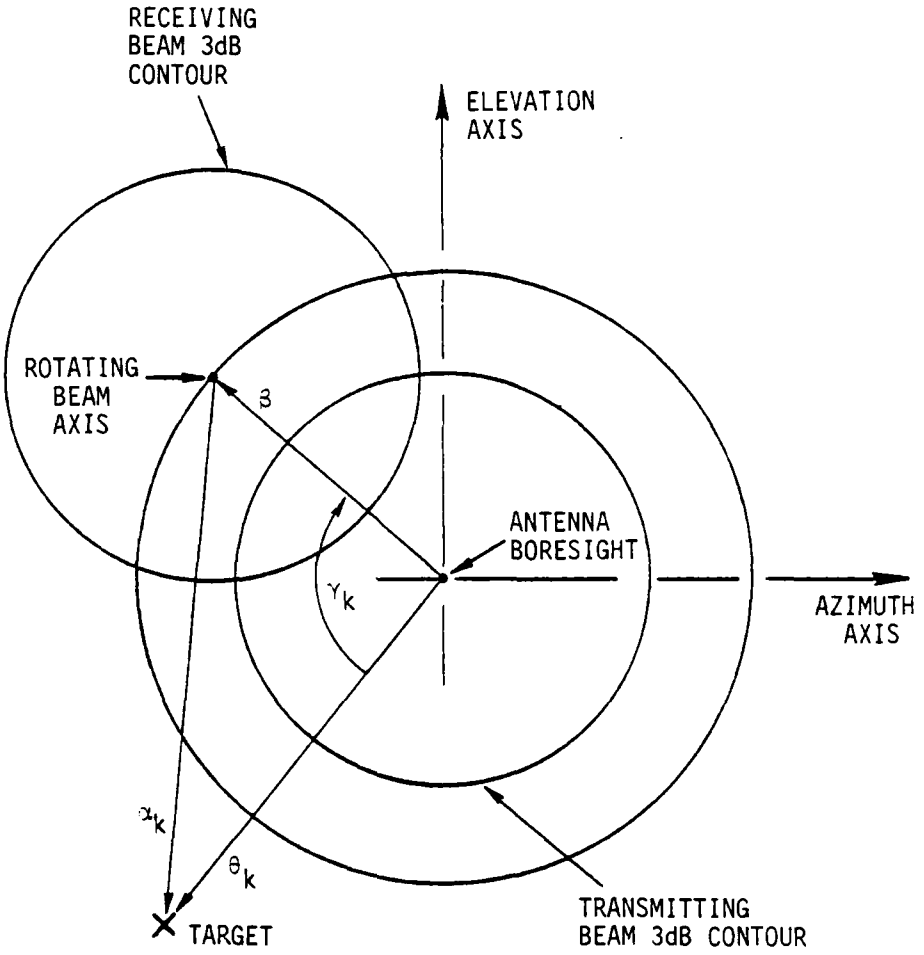

Figure 2-3. COSRO Beam Geometry

where P^T = transmitted power per pulse,

ρ_k = vector from threat to target.

The signal due to the skin return and the ECM energy emitted which is detected by the receiving beam is

$$z_k = \left|(p_k\sigma_k)^{1/2} + P_k^{ECM^{1/2}} e^{i\phi}\right|^2 A^R G^R(\alpha_k^R)[G^R(0)]^{-1}(4\pi\ |\rho_k|^2)^{-1} + w_k \tag{2.2}$$

where σ_k = target cross-section,

P_k^{ECM} = directed ECM power per pulse

A^R = effective perture of receiving beam,

G^R = gain of receiving beam.

The angle ϕ is randomly chosen from a uniform distribution between 0 and 2π. The additive noise, w_k, is Rayleigh-distributed:

$$f(w_k) = 4w_k\ \bar{w}^{-2}\ \exp\{-2w_k/\bar{w}\}\ . \tag{2.3}$$

The detected signal, z_k, then enters the AGC, the error signal filter, the error signal detector, and the servo motors. All of these signal processing models are fully described in Section 1.3. The parameter values for the standard conical scan threat are shown in Table 2-1.

2.2 SIMULATION OF ECM TECHNIQUES

The expressions for the required ECM emitter control have been developed in a previous report [2]. In order to implement them, means for computing the required signals must be developed, in particular for the average values of modulated signals.

Table 2-1. Standard COSRO Threat Parameters

THREAT COMPONENT AND PROGRAM NAME	PARAMETER	VALUE	SYMBOL	NAME
Conical Scan	Frequency	25 Hz	f_c	CSFREQ
ICSG, CGS	Phase Shift	-12°.70		
Transmitter	p.r.f.	400 Hz	f_r	PRFREQ
THRXMT	Power	200 kW	P^T	PTRANS
(Beam #2)	Squint COSRO	0°.0	β	BETA
	Squint CONSCAN	0°.6		
	Phase	0°.	γ_o	GAMMA
	Gain	40 dB	$G^T(0)$	RELGN
	Half Beamwidth COSRO	1°.5	θ_o	BMWID
	Half Beamwidth CONSCAN	1°.0		
Reciever	Squint	0°.6	β	BETA
THRRCV	Phase	0°.0	γ_o	GAMMA
(Beam #1)	Half Beamwidth	1°.0	θ_o	BMWID
	Aperture	0.88 m^2	A^R	RCVARE
	Noise	-130.0 dB	$\bar{w}$	
AGC	Gain	1.0		
AGC 5	Pole	5.0 Hz		
Error Signal Filter	Zero	10 Hz		
ERFIL	Resonant Freq.	23 Hz		
	Q	0.92		
Error Signal Detector	Averaging Period	1 Con. Scan Prd.		
AEDET	Gain	0.046		
Servos				
ISERVO2, SERVO2	Zero	1.6 Hz		
	Pole	0.16 Hz		
	Gain	200.0		

The following sections describe the computer programs which are used to simulate ECM controllers against COSRO. The ECM technique is divided into two functions: (1) the generation of a waveform, and (2) control of the waveform by a control algorithm.

2.2.1 Parametric Controller Against COSRO

The minimum-power ECM signal required to induce a constant received power at the tracking radar has been developed in [2] and is given by:

$$u_k = \frac{A_k \, E\{Y_k^2\}}{E\{Y_k\}} \left[-1 + \max_k \left[E\{G^R(\alpha_k^R)\} \right] / E\{G^R(\alpha_k^R)\} \right] . \qquad (2.4)$$

The simulation of this ECM technique consists of three parts: part one is the computation of the control voltage using the estimates for the unknown quantities, part two develops estimates for the required signals, and part three is an adaptive scheme for estimating unknown threat parameters. Each part is described below.

Because the COSRO transmitting beam does not rotate, the ESM power received per pulse does not contain as much information as the modulated CONSCAN observable. It will be assumed that there is available an additional observable, the true total tracking angle error at the time of each pulse transmission. The observables are thus:

Y_k = power received by ESM antenna on pulse k,

y_k = tracking angle error on pulse k, α_k .

The variables used in the computer program are described in Table 2-2. Some of the parameters are important properties of the threat radar, such as $\hat{\ell}$, $\hat{\beta}$, and $\hat{\theta}_o$, which are not determined adaptively by the estimation scheme. Sensitivity of the techniques to the assumed values is discussed in the performance evaluation.

Table 2-2. Variables in Programs CSRO1E.F4 and CSRO2E.F4

SYMBOL	VARIABLE	DESCRIPTION	VALUE
$\hat{\ell}$	LPULSE	Number of pulses per conical scan period	16
$\hat{\beta}$	EBETA	Estimated squint angle	0°.6
$\hat{\theta}_o$	EBWID	Estimated receiving half beamwidth	1°.0
N_d	NSETTL	Number of pulses to delay start of ECM	100
α	RISE	Angle error filter constant	0.75
θ	FMAG	Final desired angle error	0.015 rad.
α'	AFILT	ESM power filter constant	0.8
g	GAIN	Estimation technique parameter	0.0

Initialization

SYMBOL	VARIABLE	DESCRIPTION	VALUE
A_k	APLAT	Target platform constant	$A_{-1} = 500.$
θ_k	ADES	Desired angle error at time k	$\theta_{-1} = 0.0$
k	KPULSE	Pulse counter	-1
P_k	KP	Conical scan counter	1
γ_k	CSANG	Conical scan phase angle	0.0
d_γ	DCSANG	Increment to γ_k per pulse	$2\pi\ell^{-1}$
S_k	SD	Standard deviation of estimate for A_k	$S_{-2} = S_{-1} = A_{-1}$
$\bar{Y}_k$	YANG	Average received ESM power	$\bar{Y}_{-1} = 0.0$
y_k	ANG	True tracking angle error	$\theta_{-1} = 0.0$

COSRO Controller

The controller computes the power, u_k, to be applied to the ECM emitter on the kth pulse using Eq. 2.4 as a basis. The estimates used for the various quantities are:

$$A_k \rightarrow \hat{A}_k$$

$$E[Y_k^2]/E[Y_k] \rightarrow \bar{Y}_k$$

$$\max \{E[G^R(\alpha_k^R)]\} \rightarrow G(\alpha_k^{min})$$

$$E[G^R(\alpha_k^R)] \rightarrow G(\alpha_k) \ .$$

An estimate for the target platform parameter, $\hat{A}_k$, has been used instead of its true value at time k, A_k. The estimate may be either a constant chosen before the engagement begins and which does not change during the engagement (non-adaptive) or it may be determined during the engagement by an adaptive estimator. Both techniques have been implemented. Evaluations are given in Section 5.

The use of $\bar{Y}_k$, the average ESM power received per pulse, is valid in this case because Y_k is slowly varying in time, since the COSRO transmitting beam is not squinted off boresight.

The maximum receiver gain occurs when the angle between the target and beam axis, α_k^R, is a minimum. The superscript 'R' is dropped because all references will be to the receiving beam. The angle α_k^{min} is defined by

$$\alpha_k^{min} = \min_k \alpha_k^R \ . \tag{2.5}$$

Thus, the ECM power transmitted is given by

$$u_k = \begin{cases} 0 , & k < N_d \\ A_k \bar{Y}_k [-1 + G(\alpha_k^{min})/G(\alpha_k)] , & \text{otherwise} \end{cases} \quad (2.6)$$

in the computer model.

The technique employs a feedback controller because the observations, Y_k, of the radar power illuminating the target are used to adjust the strength of the ECM signal, u_k. The technique becomes adaptive when an estimation scheme is used to determine the value of $\hat{A}_k$ while the tracked radar is being controlled.

The filter for $\bar{Y}_k$ runs for N_d pulses in order to obtain a stable estimate during which no ECM power is transmitted.

COSRO Signal Generators

Each time the target is illuminated by a pulse from the tracking radar, the internal conical scan phase angle is updated by:

$$\gamma_k = \gamma_{k-1} + d\gamma , \quad (2.7)$$

and the average value for ESM power received is updated:

$$\bar{Y}_k = \alpha' \bar{Y}_{k-1} + (1-\alpha) Y_k . \quad (2.8)$$

That γ_k does not correspond to the "true" phase angle in the tracking radar is not important. It is used only to generate an ECM signal of the current frequency with the proper amplitude variation.

Once per control scan period, a new value for the desired angle error, θ_k, is obtained from the previous value and the final desired angle error, θ:

$$\theta_k = \alpha\, \theta_{k-\hat{\ell}} + (1-\alpha)\, \gamma \ . \tag{2.9}$$

The effect is to gradually increase the desired angle error from zero to its final value.

The internal version of the angle between the target and the receiving beam axis is given, for small angles, by:

$$\begin{aligned} \alpha_k^2 &= \theta_k^2 + \hat{\beta}^2 - 2\theta_k\, \hat{\beta} \cos \gamma_k \\ \alpha_k^{\min} &= |\theta_k - \hat{\beta}| \ . \end{aligned} \tag{2.10}$$

The beam shape G is then used to compute $G(\alpha_k)$ and $G(\alpha_k^{\min})$, where

$$G(\alpha) = (x^{-1} \sin x)^2 \ , \qquad x = 1.4\, \alpha\, \hat{\theta}_o^{-1} \ , \tag{2.11}$$

and $\hat{\theta}_o$ is the estimated half beamwidth.

Once the estimate, $\hat{A}_k$, is obtained, it is a simple matter to compute the ECM signal, u_k.

Adaptive Estimate for Platform Parameter

A new parameter estimate, $\hat{A}_k$, is determined only once per conical scan period, when the value of $k_m = 1 + k \bmod \hat{\ell} = 1$. That estimate is then used throughout the next conical scan period to generate the ECM signal. When $k_m = 1$ and $k \geq N_d$,

$$P_k = P_{k-1} + 1 \ , \tag{2.12}$$

and a new estimate, $\hat{A}_k$, is computed by comparing the desired angle error, θ_k, with the actual angle error, y_k:

$$\hat{A}_k = \hat{A}_{k-\hat{\ell}} - \frac{P_{k-2}}{P_{k-1}} S_{k-2\hat{\ell}}\, g\left(1 - \frac{y_{k-\hat{\ell}}}{\theta_k}\right) + S_{k-\hat{\ell}} \left(1 - \frac{y_k}{\theta_k}\right), \qquad (2.13)$$

where: $S_k^2 = S_{k-\hat{\ell}}^2 (P_{k-\hat{\ell}}/P_k)[1 + P_k^{-1}(1 - y_k/\theta_k)^2]$.

Parametric Controller: Non-Adaptive ECM Technique Against COSRO

This ECM technique is very similar to the adaptive technique described above but no attempt is made to ascertain the value of the platform parameter, A_k, during the encounter. Instead, a pre-specified value of $A_k = A_o$ is used throughout the engagement. The controller still employs feedback through the use of its observations, Y_k and y_k to adjust for illumination by the tracking radar.

The input parameters are the same as in Table 2-2 except that $A_k = A_o = 500.0$ is also included. Since no estimation technique is employed, S_k is not used. The initialization is otherwise the same as in Table 2-2.

2.2.2 Input/Output Controller Interface for COSRO

Two techniques were used to interface the jamming module with controllers designed for linear systems. Both techniques use the actual radar boresight angular error (with additive gaussian noise if desired) as the state parameter y. As each new value of y is presented to a controller (or identifier-controller pair) the controller computes a new control u which is used to control the ECM signal transmitted during the next sampling interval.

A reference signal is used which is modulated at the radar's conical scan frequency. Both of the interface techniques described here use sinusoidal modulation at exactly the scan frequency. The assumption is that the scan rate is fixed and known. For the "depth modulation" technique the power to be transmitted as ECM during pulse k is given as a function of u:

$$\text{ECMPOW}_k = 1 - u \sin(2\pi k/\hat{\ell}) ,$$

where $\hat{\ell}$ is the number of pulses per conical scan. For the "amplitude modulation" technique:

$$ECMPOW_k = |u| - u \sin(2\pi k/\hat{\ell}) \ .$$

Sampling

ECM power is generally transmitted on each pulse thus requiring one of the above calculations to be performed for each pulse. However, it is undesirable to sample the angle error y for use in identification and computation of u (the control parameter) at a rate faster than the dynamics of the radar system. Thus some subsampling is required. It is also apparent from the modulation equations that u should be held constant for a multiple of $\hat{\ell}$ pulses (integer number of conical scans). In general with the ARMA based controllers which have been implemented against the "standard" threat a sampling interval of $2\hat{\ell}$ pulses has been satisfactory.

Ramping

It has been found that when control is first applied to the radar it is advantageous to preempt drastic control commands which can cause the radar to lose track or behave erratically. This is particularly true if no identification phase is used or if this phase is short. For identification/control mechanisms this is easily accomplished by smoothly adjusting Y_{REF} (desired boresight angle error) from zero (identification phase) to its final value. An exponential ramp with a time constant of approximately 1 second is generally adequate.

For certain direct controllers such as output matching, no identification phase is involved which means that no estimate of the closed loop gain of the system is available to startup. In this case, it is desirable to limit the control in the beginning. Note also that since the depth modulation technique transmits a constant average power (typically 10 dB or so above the skin return) it is desirable to smoothly turn the ECM power up when using this technique. These goals are easily accomplished by limiting the ECM power transmitted to the level of an exponential ramp as used above for Y_{REF}.

3. PSUEDO-MONOPULSE SYSTEMS

A psuedo-monopulse system consists of two radar beams, π radians out of phase, each squinted off the antenna axis by angle θ, which are either electrically or mechanically rotated about the antenna axis. One of the beams transmits and both of them receive. The beam configuration is shown in Figure 3-1. The following sections describe the standard threat model and the ECM techniques which have been developed.

3.1 PSUEDO-MONOPULSE TRACKING LOOP

The block diagram of the simulation for psuedo-monopulse threat model is shown in Figure 3-2. The major signal processing functions are shown along with the interface between the threat and target models.

The beam geometry, shown in Figure 3-1, requires that two beams be defined. One is the main beam, which both transmits and receives. The other is the auxiliary beam, which only receives.

The transmitted power density illuminating the target is given by

$$p_k = P^T G^T(\alpha_k^T) \ (4\pi \ |\rho_k|^2)^{-1} \ , \tag{3.1}$$

where: P^T = transmitted power per pulse,

G^T = main beam gain,

α_k^T = angle of target from main beam axis,

ρ_k = range to target.

The signals detected by each beam have contributions from both the power reflected from the target and from ECM power:

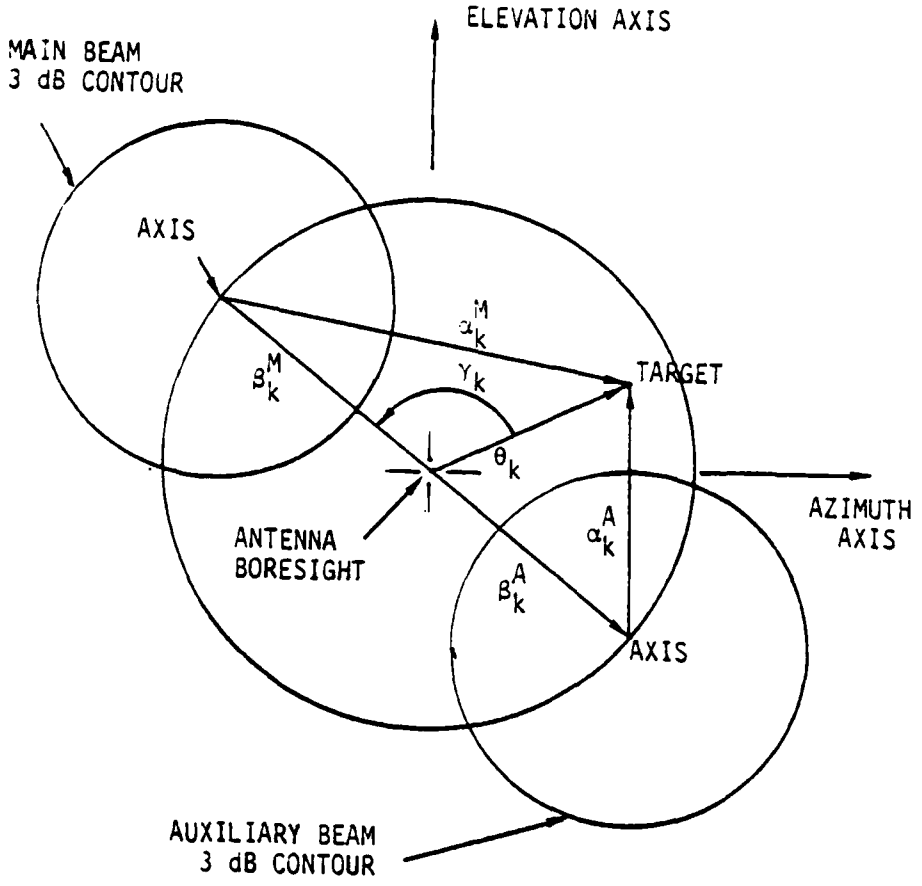

Figure 3-1. Psuedo-monopulse Beam Geometry

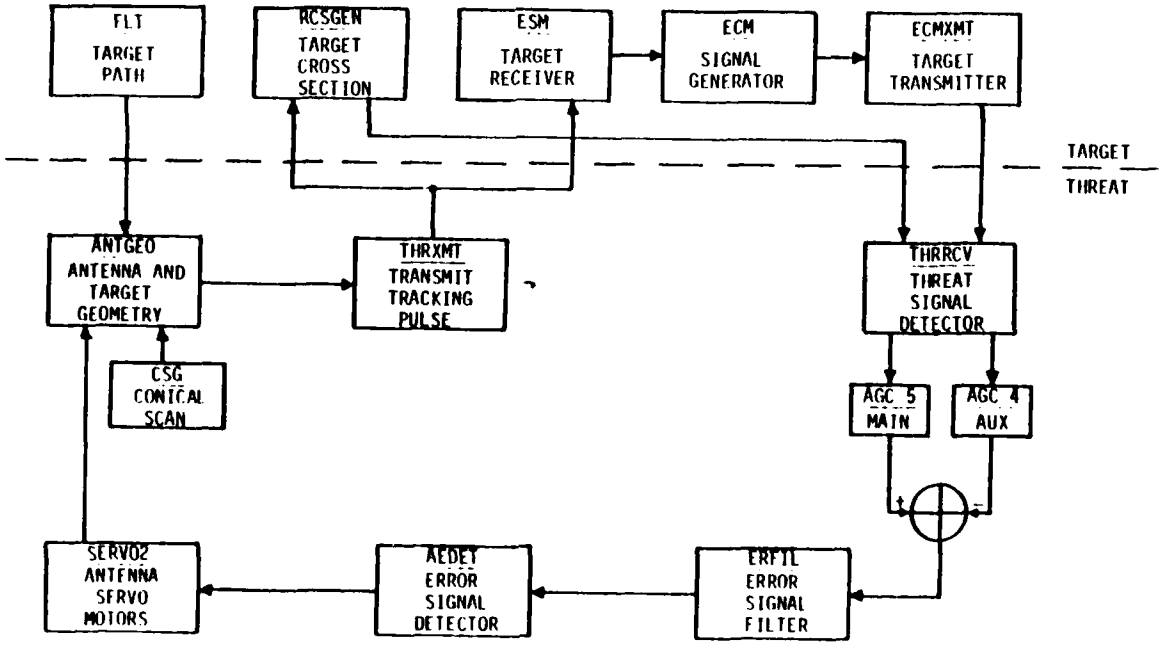

Figure 3-2 Psuedo-monopulse Threat Model Block Diagram Showing Program Names

$$Z_k^B = \left| (p_k \sigma_k)^{1/2} + P_k^{ECM\,1/2} e^{i\phi} \right|^2 A^B G^B(\alpha_k^B) \; [G^B(0)]^{-1} (4\pi \; |\rho_k|^2)^{-1} + w_k \; , \tag{3.2}$$

where:
- σ_k = target cross-section,
- P_k^{ECM} = directed ECM power per pulse,
- A^B = effective aperture,
- G^B = gain of beam,
- α_k^B = angle of target from beam axis,
- B = main (T) or auxiliary (R) beam.

The angle ϕ is randomly chosen from a uniform distribution on the interval $[0,2\pi]$. The additive noise, w_k, is chosen from a Rayleigh distribution (see Eq. 2.3).

Each of the detected signals enters an AGC. The difference of the AGC outputs enters an error signal filter, the error signal detector, and the servo motors. All of these signal processing models are fully described in Section 1.3. The parameter values for the standard psuedo-monopulse threat model are shown in Table 3-1.

3.2 SIMULATION OF ECM TECHNIQUES

The expressions for the required ECM emitter control have been developed and analyzed in [2]. The following sections describe the computer programs which are used to simulate ECM controllers against psuedo-monopulse. Again each ECM technique is divided into: (1) the generator of a waveform, and (2) the control of the waveform parameters.

3.2.1 Parametric Controller Against Psuedo-monopulse

The control is the voltage, u_k, of the ECM emitter on the kth pulse. The periodic waveform is:

Table 3-1. Standard Psuedo-monopulse Threat Model Parameters

THREAT COMPONENT AND PROGRAM NAME	PARAMETER	VALUE	SYMBOL	NAME
Conical Scan	Frequency	25 Hz	f_c	CSFREQ
ICSG, CSG	Phase Shift	-13°.29	ϕ_{REF}	
Transmitter	p.r.f.	400 Hz	f_r	PRFREQ
THRXMT	Power/Pulse	200 kW	P^T	PTRANS
(Beam #2)	Squint angle	0°.6	β	BETA
	Phase	180°	γ_o	GAMMA
	Gain	40 dB	$G^T(0)$	RELGN
	Half Beamwidth	1°.0	θ_o	BMWID
	Aperture	0.88 m^2		
Receiver	Squint angle	0°.6	β	BETA
THRRCV	Phase	0°.0	γ_o	GAMMA
	Half beamwidth	1°.0	θ_o	BMWID
	Aperture	0.88 m^2		
	Noise	-130.0 dB	$\bar{w}$	ANOISE
AGC	Gain	1.0		
AGC4, AGC5	Pole	0.5 Hz		
Error Signal Filter	Zero	10. Hz		
ERFIL	Resonant freq.	23. Hz		
	Q	0.92		
Error Signal Detector	Averaging Period	1 Conical Scan Period		
AEDET	Gain	0.023		
Servos	Zero	1.6 Hz		
1SERV2, SERVO2	Pole	0.16 Hz		
	Gain	200.0		

$$u_k = \begin{cases} 0 & , \quad k \leq N_d \\ S_k \, \delta(k \bmod i) & , \quad \text{otherwise} \end{cases} \tag{3.3}$$

where N_d is a delay before the ECM is turned on and S_k is the emitted amplitude. The waveform has period i.

The amplitude of the emitted pulse, S_k, is controlled by the output of a filter whose input, y_k, is the true observed tracking angle error on the kth pulse:

$$\bar{y}_k = \alpha_s \bar{y}_{k-1} + (1 - \alpha_s) y_k \, . \tag{3.4}$$

The amplitude is feedback-controlled according to

$$S_k = S^{ECM} \, e^{-\bar{y}_k^2 \theta_o^{-2}} \, , \tag{3.5}$$

where S^{ECM} is a constant and θ_o is a parameter representing the half-beamwidth of the tracking radar. The parameters for the parametric controller against psuedo-monopulse are shown in Table 3-2.

3.2.2 Input/Output Controller Interfaces

As in the COSRO simulation the observable radar state parameter y is taken to be the actual boresight angular error of the pseudo-monopulse radar. A simple one pole smoothing filter is used with a time constant of 200 pulses to smooth the rather irregular behavior of this parameter. This smoothed estimate is sampled and fed to the desired identification/control setup which then computes a new control u to be used during the next sampling interval. The sampling interval chosen for this process (see Section 2.2.2) is 120 pulses/sample.

The actual waveform transmitted as ECM is defined in Section 3.2.1, Eq. (3.3). The pulse amplitude S_k of the pulse is determined from the control value u by:

Table 3-2. Description of Variables in Parameteric Controller Against Psuedo-Monopulse

SYMBOL	VARIABLE	VALUE	DESCRIPTION
α	ALFCOM	0.0	Comb filter constant
N_d	NSETTL	100	Number of pulses to delay start of ECM
$\hat{\ell}$	LHAT	16	Estimated number of pulses in conical scan period
θ_o	EBWID		Estimated half beamwidth
S^{ECM}	SECM	1000.0	ECM voltage
i	IECM	9	ECM pulse spacing
α_s	SFILT	0.995	Angle error filter parameter
k	KPULSE	-1	Pulse counter
$\bar{\theta}_k$	SANGER	0.0	Filtered angle error
k_ℓ	KMODL		Estimated conical scan pulse position
k_i	KMODE		Pulse number relative to ECM pulse spacing
θ_k	YK(2)		Observed true tracking angle error
y_k	YK(1)		Observed ESM power received

$$S_k^2 = (u + u_{BIAS})(1. - .99^k) \ .$$

The second term in the above product is simply an exponential ramp as used against COSRO. The u_{BIAS} term is an estimate of the "critical u" at which the radar is just becoming unstable. This term is not really necessary for certain controllers which can determine the bias term themselves.

4. MONOPULSE SYSTEMS

A monopulse system has at least two feed horns in the tracking direction which are not rotated, but rather sense the wavefront distortion coherently, resulting in an error signal. The particular monopulse system simulated is a full three-channel amplitude comparison monopulse.

This section describes the monopulse threat model and the ECM techniques which have been developed to counter this threat.

4.1 MONOPULSE THREAT TRACKING LOOP

The monopulse threat model is intended to represent the behavior or a true, three-channel monopulse antenna, although the parameters used do not represent a particular system. The monopulse model differs from the conical scanning systems, with or without compensation, in that a spatially extended target is required. The associated geometry has been described in Section 1.2.3.

The block diagram for simulation of the monopulse radar is shown in Figure 4-1, which includes the program names and the interface to the target model.

There are four beams defined for the antenna, each squinted off-axis by the same amount and located at phase angles corresponding to the azimuth and elevation axes, as shown in Figure 4-2.

The power density at the target transmitted by the tracking radar is

$$P_k = P^T \left[\tfrac{1}{4} \sum_{j=1}^{4} G^{(j)}(\alpha_k^{(j)}) \right] (4\pi \ |\rho_k|^2)^{-1} \ , \qquad (4.1)$$

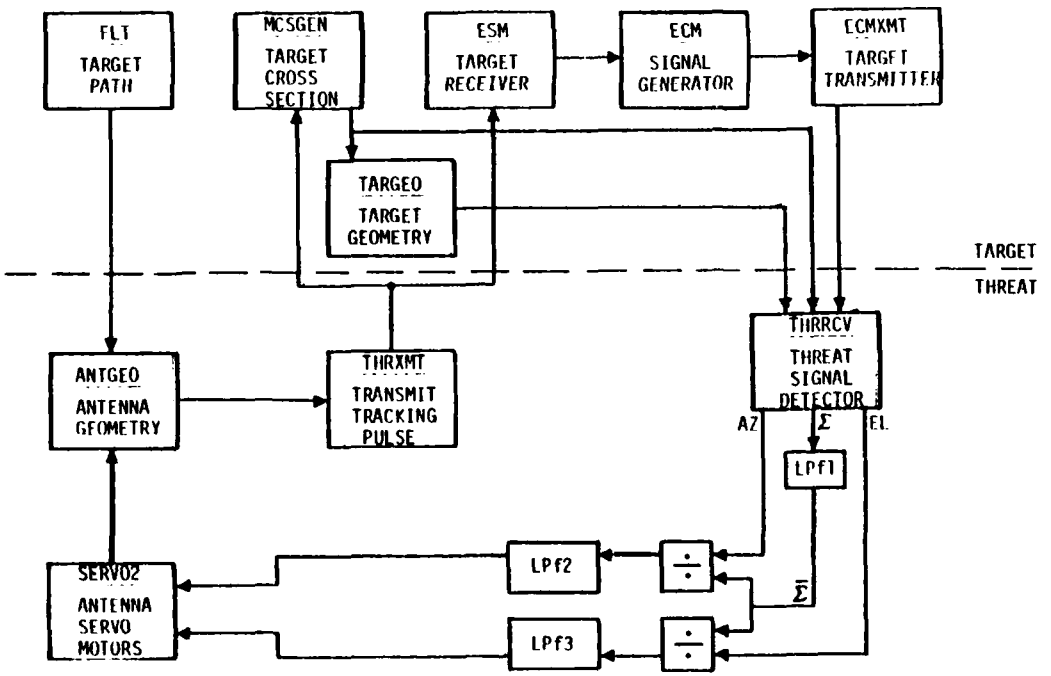

Figure 4-1. Monopulse Threat Model Block Diagram Showing Program Names

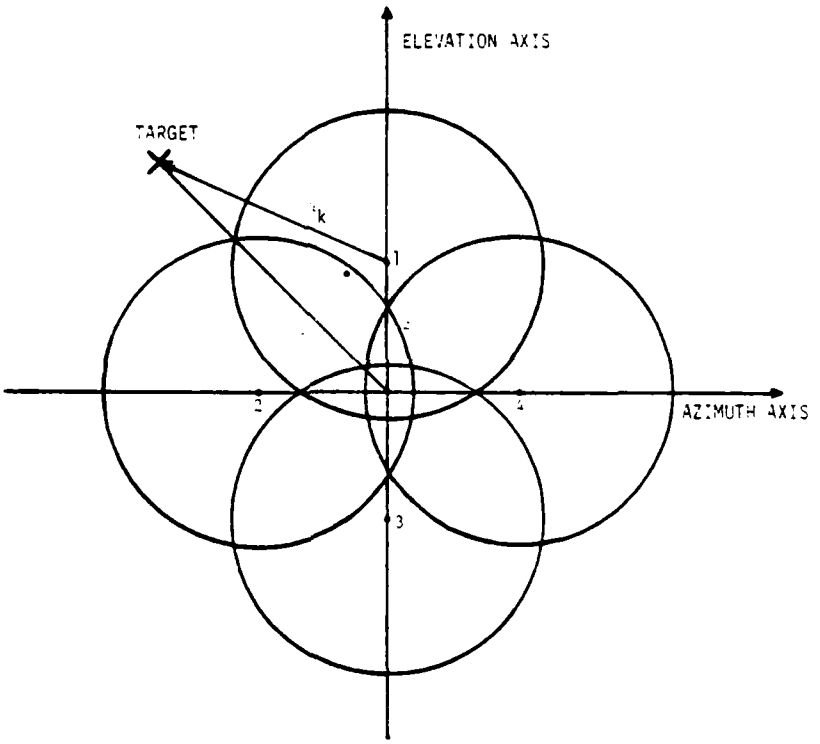

Figure 4-2 Monopulse Beam Geometry

where: P^T = power transmitted per pulse,

$G^{(j)}$ = gain of jth beam,

$\alpha_k^{(j)}$ = angle of target from jth beam axis,

ρ_k = vector from threat to target.

An extended target is modeled as a set of point sources (scatterers or emitters), each characterized by an amplitude a_i and phase ϕ_i. The amplitude is

$$a_i = \begin{cases} [\sigma_k(i) \cdot p_k \cdot g(\alpha_k(i))]^{1/2} & \text{scatterer} \\ [u_k(i) \cdot g(\alpha_k(i))]^{1/2} & \text{emitter} \end{cases} \tag{4.2}$$

where g is the relative gain of the receiving beam normalized to 1 on-axis, and $\alpha_k(i)$ is the angle of the source off antenna boresight. The phase of the ECM emitters is determined by the controller. For scatterers, ϕ_i can be either fixed or chosen uniformly on the interval $[0,2\pi]$.

The signal received in the ℓth channel is

$$S_\ell = A(4\pi |\rho_k|^2)^{-1} \sum_{ij} f_i^\ell a_i a_j \cos[\phi_i - \phi_j - 2\pi K(\Delta_i - \Delta_j)] + w_k \ , \tag{4.3}$$

where

$$f_i^\ell = \begin{cases} 1 & \ell = \text{sum channel} \\ y_k^{Az}(i) & \ell = \text{azimuth channel} \\ y_k^{EL}(i) & \ell = \text{elevation channel,} \end{cases}$$

A = antenna effective aperture,

Δ_i = range to ith source,

$K = \lambda^{-1}$, λ is transmitted wavelength.

The noise, w_k, is Rayleigh distributed (see Eq. 2.3).

The sum-channel signal enters a low-pass filter whose output is used to control the gain of the azimuth and elevation channels. Those gain-controlled signals are then filtered and used to drive to the servo motors. The parameters of the standard monopulse threat model are shown in Table 4-1.

4.2 SIMULATION OF ECM TECHNIQUES

Input/Output Interface for Monopulse

The observable parameter for the monopulse radar simulation is the azimuth component of the pointing error. This is in contrast to the COSRO and pseudo-monopulse simulations in which the observable (y) is the total angular error. This value is subsampled by a factor of 30 and used to compute a control parameter u by the identification/control scheme selected. This value is then used to compute the amplitude and phase of ECM transmitted from each of 2 antennas during the next 30 pulses.

First the control is "linearized" by defining a gain term A:

$$A = \left|\frac{u^*+1}{u^*-1}\right|, \quad \text{where} \quad u^* = \begin{cases} u & \text{if } \left||u|-1\right| < .4 \\ 1.4\,\mathrm{SGN}(u) & \text{otherwise.} \end{cases}$$

A phase is also computed:

$$\phi = 2\pi \cdot \mathrm{WAVNUM} \cdot \Delta R + \begin{cases} \pi & \text{if } |u| > 1. \\ 0 & \text{otherwise,} \end{cases}$$

where WAVNUM is the wave number of the output and ΔR is the difference in range of the radar from the two ECM antennas. This equation means that the output from the two antennas will arrive at the radar with a phase difference of π if $|u| > 1.$ and ϕ if $|u| \leq 1.$
Now the amplitude and phase of the output can be written:

$\mathrm{AMP}(1) = 1.$
$\mathrm{AMP}(2) = A \cdot \mathrm{AMP}(1)$
$\mathrm{PHASE}(1) = 0.$
$\mathrm{PHASE}(2) = \phi$

Table 4-1. Standard Monopulse Threat Model Parameters

THREAT COMPONENT AND PROGRAM NAME	PARAMETER	VALUE	SYMBOL	NAME
Transmitter	p.r.f.	400 Hz	f_r	PRFREQ
THRXMT	Power/pulse	200 kW	P^T	PTRANS
	Squint angle	0°.6	β	BETA
	Phase	0°,90°,180°, 270°	γ_o	GAMMA
	Gain	40 dB		GNAXIS
	Half beamwidth	1°.0	θ_o	BMWID
Reciever	Noise	-130 dB	$\bar{w}$	ANOISE
THRRCV	λ^{-1}	10 m^{-1}	K	WVNMBR
	Aperture	0.88 m^2	A	RCVARE
Sum Channel	Gain	10.0		
ILPF1, LPF1	Freq. Cutoff	2.0 Hz		
Azimuth Channel	Gain	10.0		
ILPF2, LPF2	Freq. Cutoff	2.0 Hz		
Elevation Channel	Gain	10.0		
ILPF3, LPF3	Freq. Cutoff	2.0 Hz		
Servos	Zero	1.6 Hz		
	Pole	0.16 Hz		
	Gain	200.0		

5. SAMPLE RUNS

The simulation of the adaptive closed-loop ECM techniques described herein accomplished the primary objective of algorithm development. That is, the algorithms described in [2] and this report were developed in part by using the simulation to understand ECM behavior. There was never any intention to use the current simulation for "production runs". Early sample runs of the simulation are meaningless for technique evaluation. Therefore the limited number of sample runs given in this section utilize the algorithms in their final forms (as described in Sections 2 through 4).

As the controllers will be developed further in subsequent phases of the program, even those runs presented herein are not indicative of the ultimate gains to be achieved using adaptive closed-loop control techniques. For this reason only a sampling of the runs is presented. They are meant to be representative of the performance of the techniques at the current time, and contain a variety of parameters, methods, and tests. Definitive conclusions from such runs generated by the simulation will be given during the next phase of the program, when algorithms will be developed to work against actual threat radar systems.

Sample runs are given against all three radar systems: COSRO in Section 5.1, psuedo-monopulse in Section 5.2, and monopulse in Section 5.3. Parametric controller results are shown against COSRO and psuedo-monopulse, and input/output model controllers are shown against COSRO and monopulse. These choices are due to the following considerations. COSRO is the simplest system, due to its direct coupling of observation and ECM and its nearly linear structure. Thus parametric and input/output controllers were developed against COSRO. The emphasis on COSRO is not so much indicative of threat system importance, but rather shows the "walk before you run" research performed under the current project. Then a significant amount of analysis (see [2]) was performed to understand the technique used against psuedo-monopulse, and only later was the control tried. The first controller tried with the new technique was the parametric controller. Meanwhile, the input/output controller work emphasized monopulse.

In all cases only brief descriptions are given of the controllers, and there is no attempt at global conclusions, due to the developmental nature of the algorithms. In all cases the controllers "worked", in the sense that they induced the error behavior desired. This control of the threat radar indicates the power in the approach.

5.1 SAMPLE RUNS AGAINST COSRO

Since most of the algorithm development was done for the COSRO radar, the most sample runs are presented. Table 5-1 describes the sample runs, with Figures 5-1 through 5-20 giving outputs. In this and subsequent tables the plot types are given by:

1 - Angle error versus time at start of ECM

2 - Angle error histogram at start of ECM

3 - Angle error versus time in steady-state

4 - Angle error versus histogram in steady-state

5 - ECM signal versus time (envelope)

6 - ECM histogram

7 - Skin return versus time

8 - Skin return histogram

9 - Azimuth or elevation angle error

10 - Psuedo-monopulse error signal.

Not all plot types are represented, but at some time during algorithm development they were all examined.

Figures 5-1 and 5-2 give baseline results for COSRO when no ECM is applied. Figures 5-3 through 5-9 are sample runs for the parametric controller (see Section 2.2.1). Figures 5-3 through 5-6 give results for the adaptive controller. Figures 5-7 and 5-8 give results for the nonadaptive controller when differing a priori information is given. In Figure 5-7 the parameter A, which has a value 500 for this radar model, is given correctly to the controller.

In contrast, Figure 5-8 shows the angle error when the parameter A is given incorrectly as 1250. The adaptive controller, assuming no prior knowledge of A (set equal to zero), takes longer to settle to near the reference angle, as expected; see Figure 5-9.

Figures 5-10 through 5-20 are sample runs for the input/output controllers (see Section 2.2.2). Figures 5-10 through 5-12 are samples for the three different controllers, certainty equivalence (CE), cautious, and dual, all with real-time least squares (RTLS) identification. An initial identification-only phase is done on all runs. Figures 5-13 through 5-18 show comparisons of differing techniques with a nonscintillating target, so only controller errors are shown. Figure 5-13 is an open-loop (step) control sample. Figures 5-14 through 5-16 are the three controllers with RTLS, while Figures 5-17 and 5-18 are the cautious and dual controllers with recursive instrumental variable (RIV) identification. (The CE controller was virtually identical to the cautious controller.) Figures 5-19 and 5-20 show two sample runs for the controller that destabilizes the radar at a controlled rate. Cautious control with RTLS was used.

Table 5-1. Sample Runs Against COSRO

FIGURE	PLOT TYPE	REFERENCE ANGLE	CONTROLLER
5-1	7	-	No ECM
5-2	1	-	No ECM
5-3	5	0.3 BW	Adaptive parametric
5-4	1	0.3 BW	Adaptive parametric
5-5	3	0.3 BW	Adaptive parametric
5-6	6	0.3 BW	Adaptive parametric
5-7	1	0.3 BW	Nonadaptive parametric (see Note 1)
5-8	1	0.3 BW	Nonadaptive parametric (see Note 2)
5-9	1	0.3 BW	Adaptive parametric (see Note 3)
5-10	1	10 mrad	CE with RTLS (see Note 4)
5-11	1	10 mrad	Cautious with RTLS (see Note 4)
5-12	1	10 mrad	Dual with RTLS (see Note 4)
5-13	1	-	Open-loop (see Note 5)
5-14	1	10 mrad	CE with RTLS (see Notes 4 and 5)
5-15	1	10 mrad	Cautious with RTLS (see Notes 4 and 5)
5-16	1	10 mrad	Dual with RTLS (see Notes 4 and 5)
5-17	1	10 mrad	Cautious with RIV (see Notes 4 and 5)
5-18	1	10 mrad	Dual with RIV (see Notes 4 and 5)
5-19	1	Destabilization	Cautious with RTLS (see Note 6)
5-20	1	Destabilization	Cautious with RTLS (see Note 6)

Notes

1 - $A = 500$, $\hat{A} = 500$.

2 - $A = 500$, $\hat{A} = 1250$.

3 - $A = 500$, $\hat{A} = 0$.

4 - Identification only until pulse number 100.

5 - Target not scintillating.

6 - Identification only until pulse number 200.

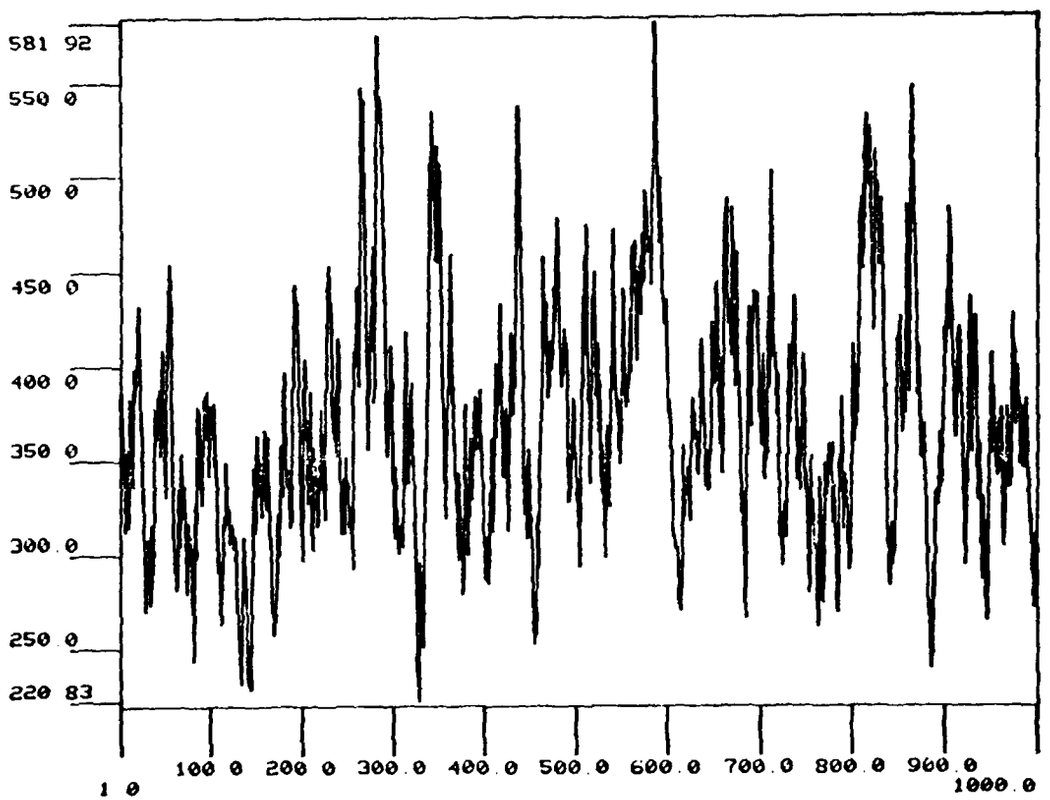

Figure 5-1. Skin Return - No ECM - COSRO

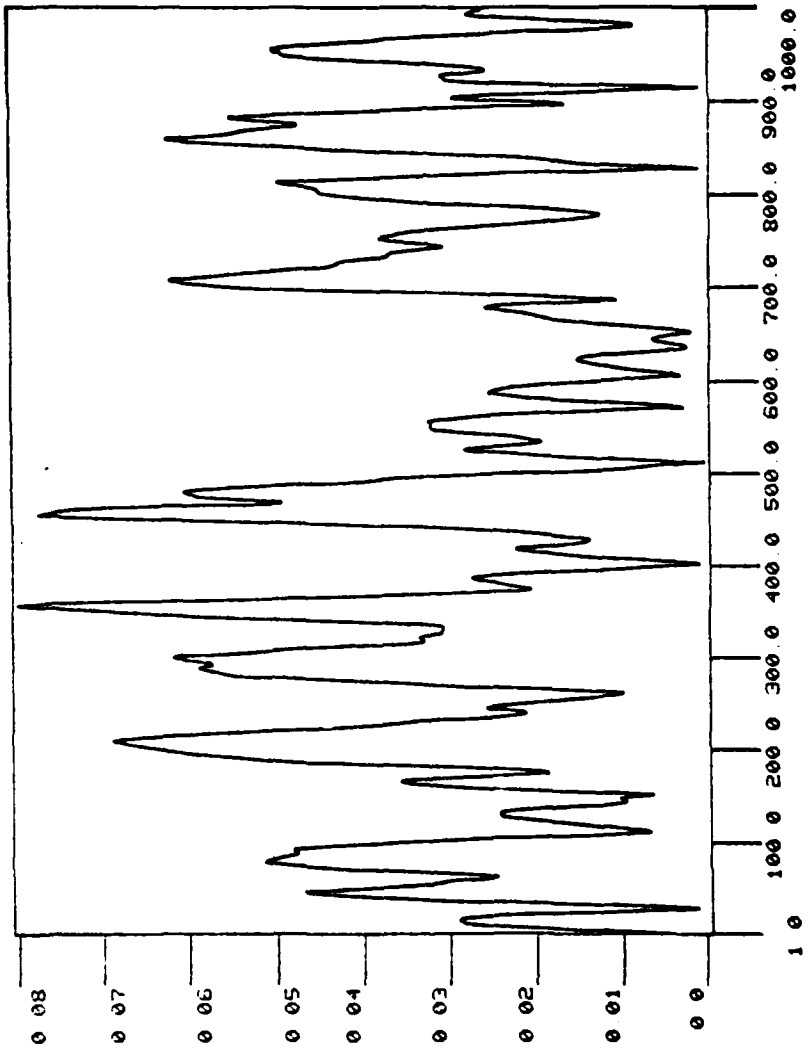

Figure 5-2. Angle Error - No ECM - COSRO

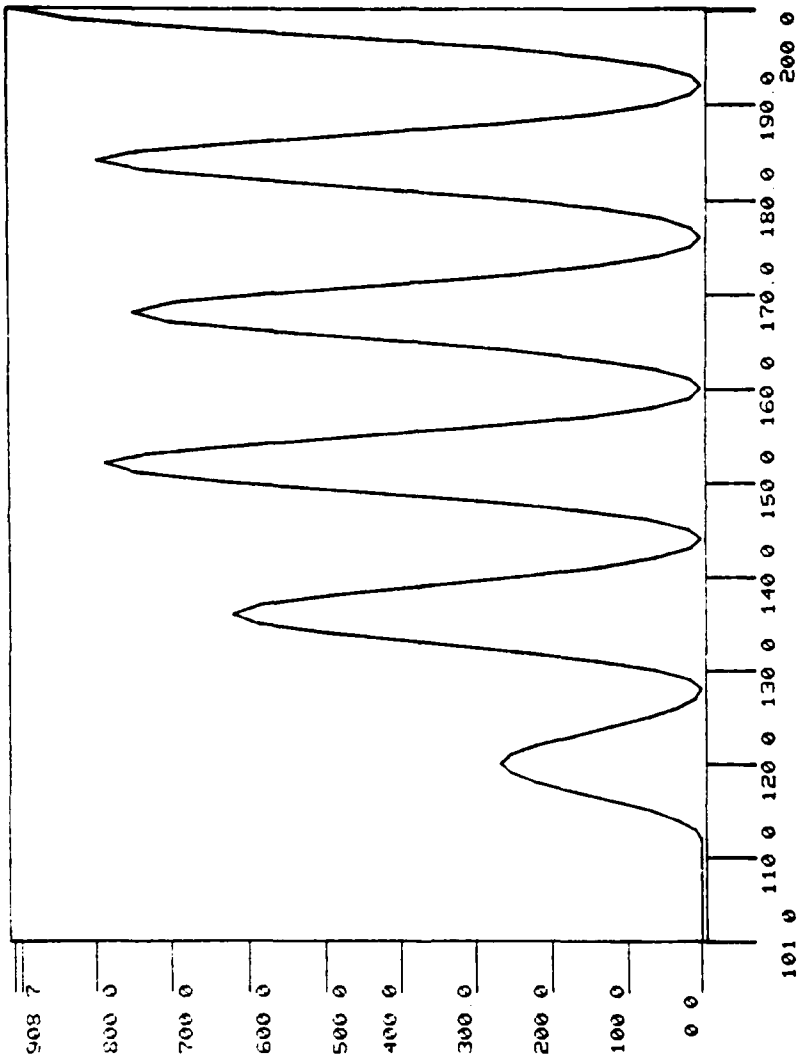

Figure 5-3. ECM Signal - Adaptive Parametric Controller - COSRO

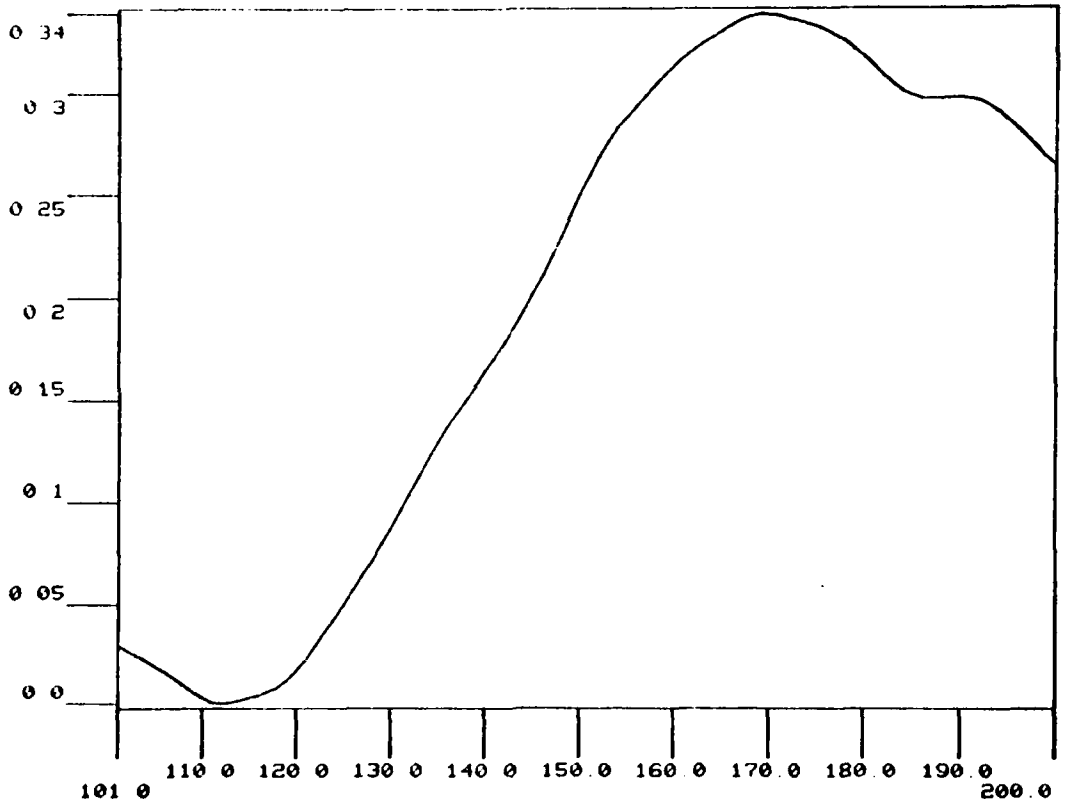

Figure 5-4. Angle Error - Adaptive Parametric Controller - COSRO

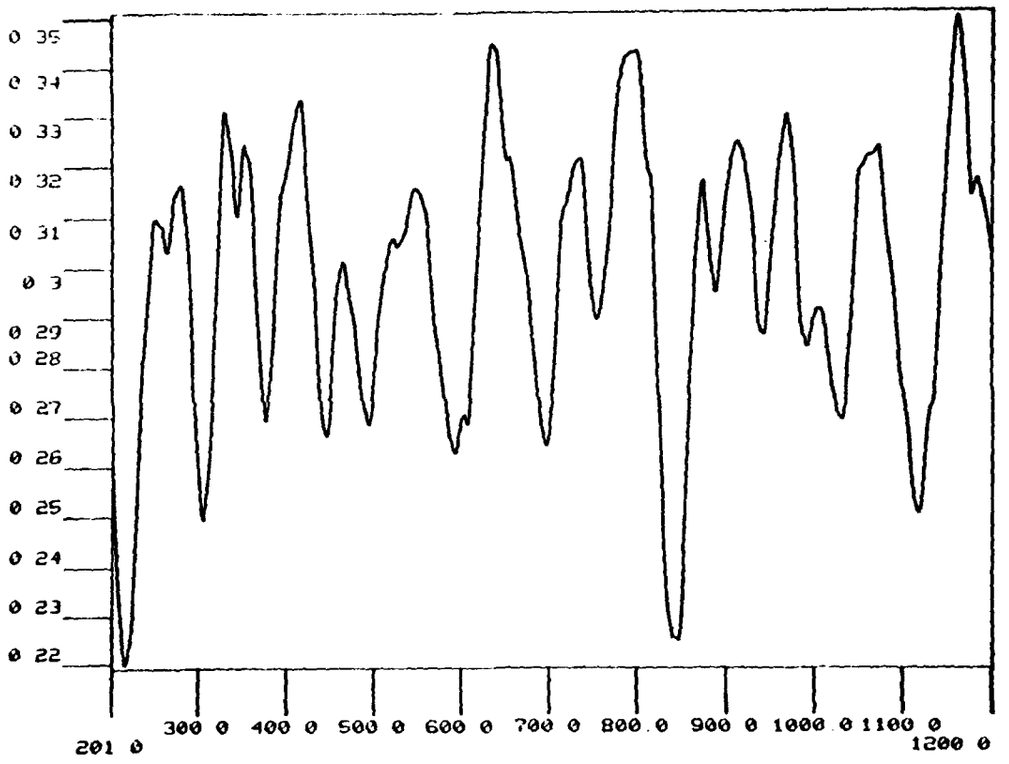

Figure 5-5. Angle Error - Adpative Parametric Controller - COSRO

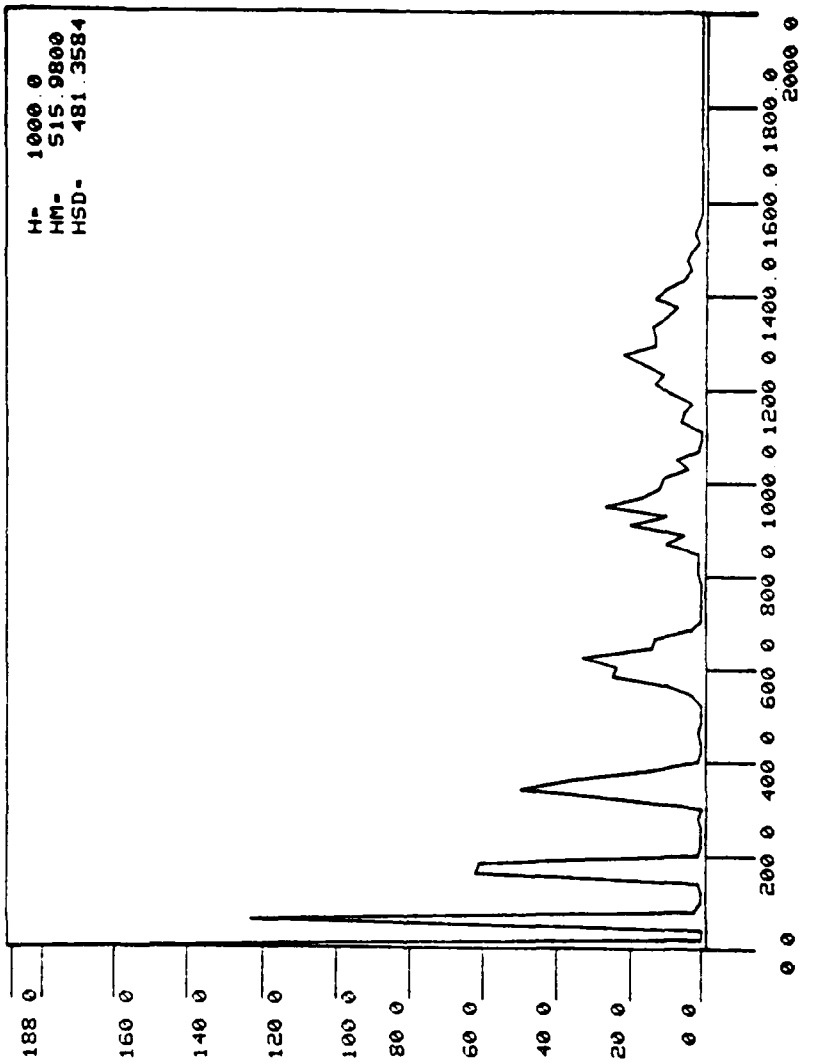

Figure 5-6. ECM Histogram - Adpative Parametric Controller - COSRO

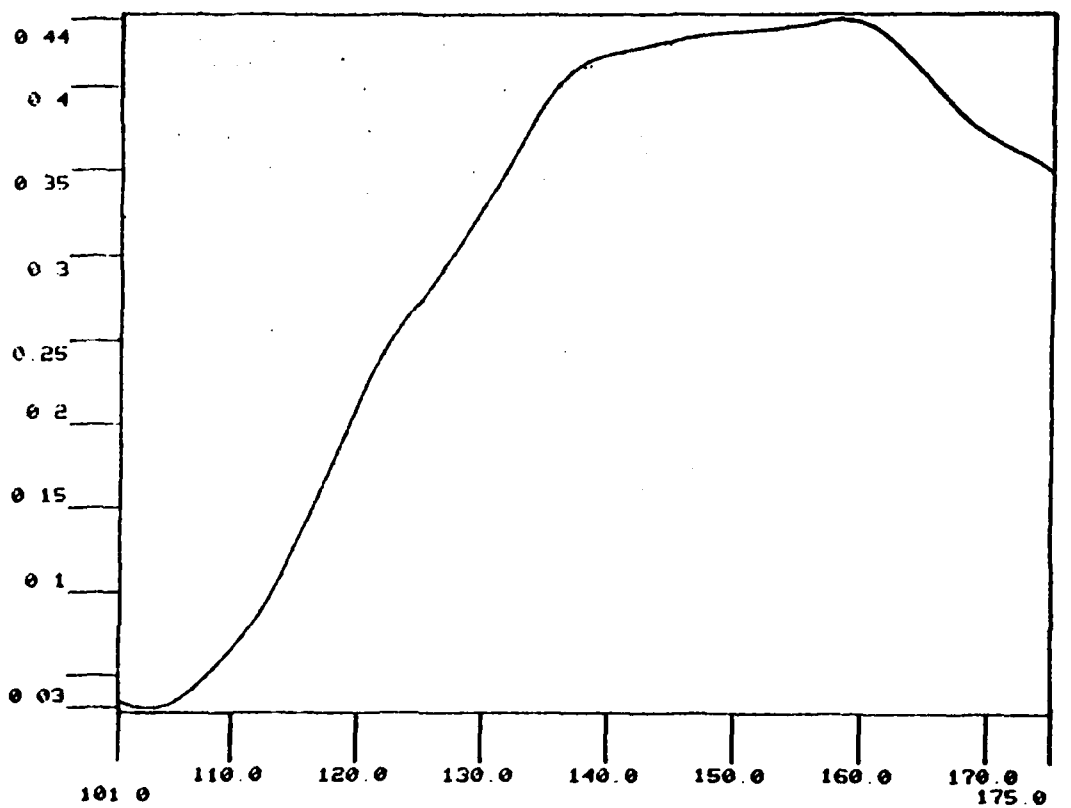

Figure 5-7. Angle Error - Nonadaptive Parametric Controller - $\hat{A} = 500$ - COSRO

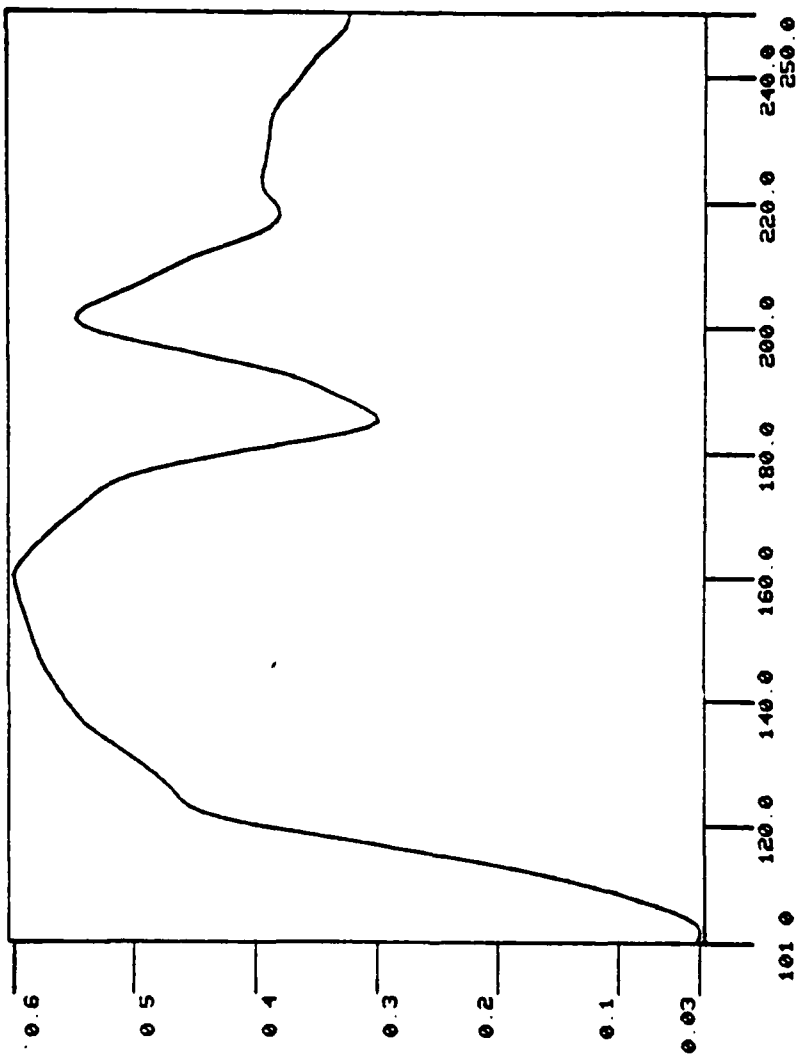

Figure 5-8. Angle Error - Nonadaptive Parametric Controller, $\hat{A} = 1250$ - COSRO

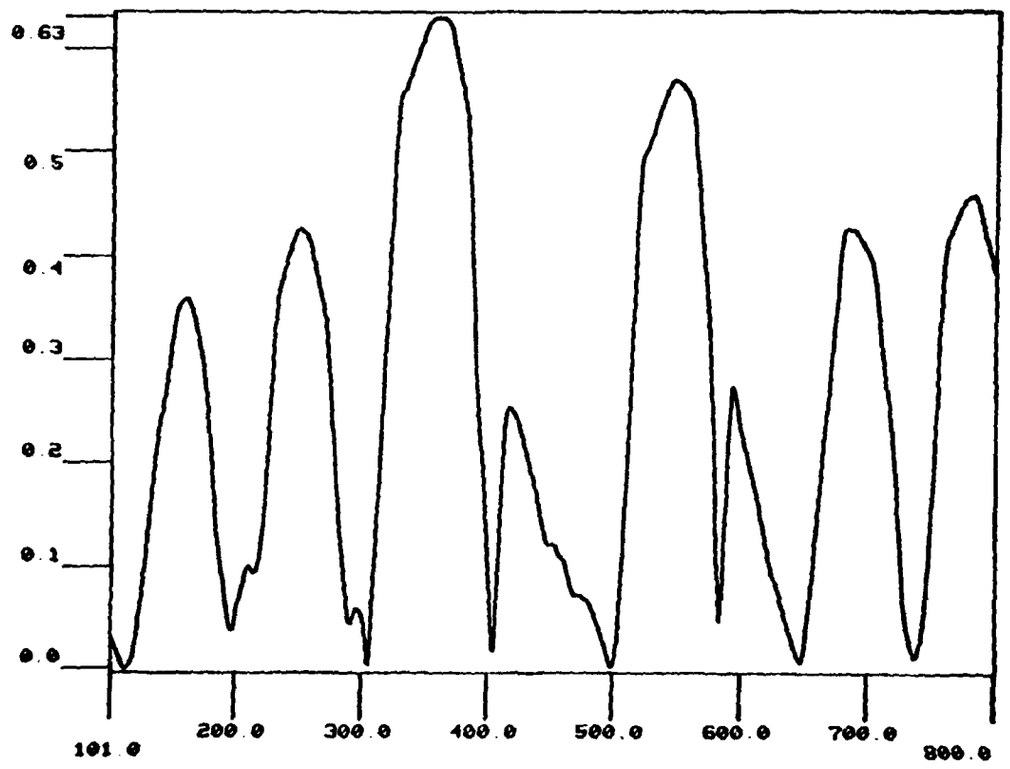

Figure 5-9. Angle Error - Adaptive Parametric Controller, $\hat{A} = 0$ - COSRO

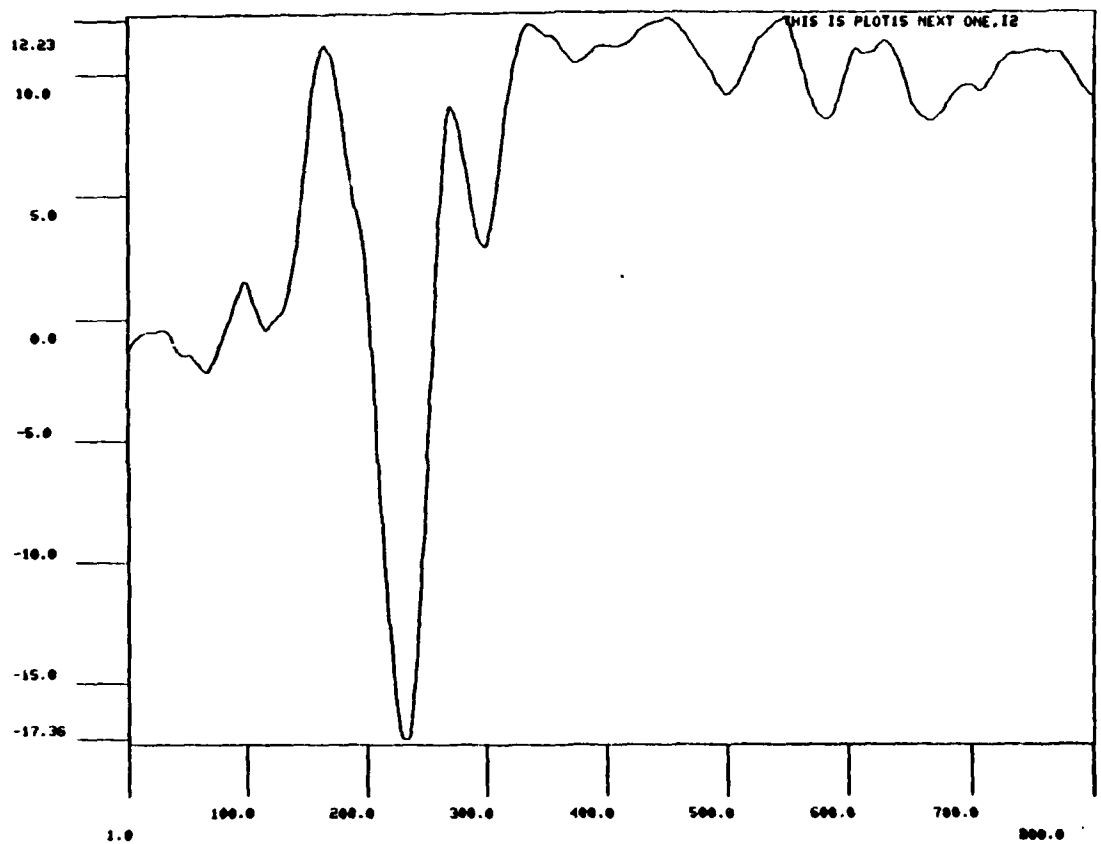

Figure 5-10. Angle Error - CE/RTLS Controller - COSRO

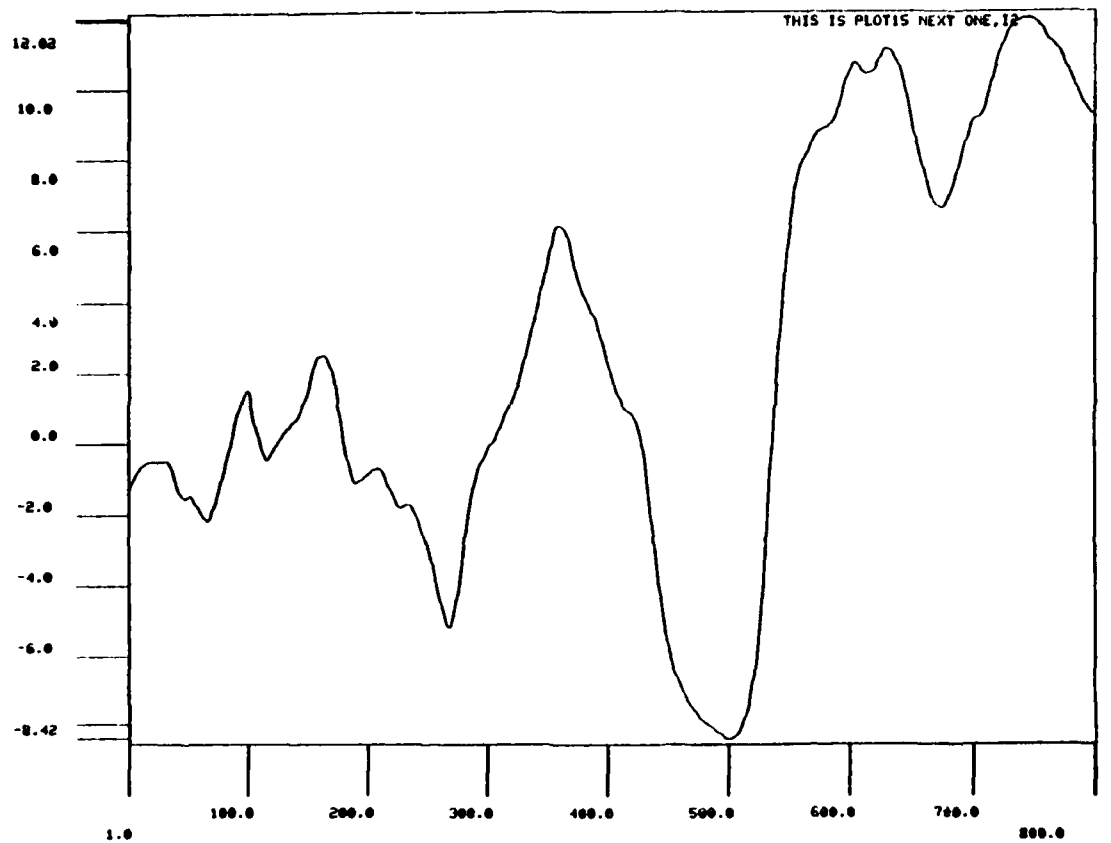

Figure 5-11. Angle Error - Cautious/RTLS Controller - COSRO

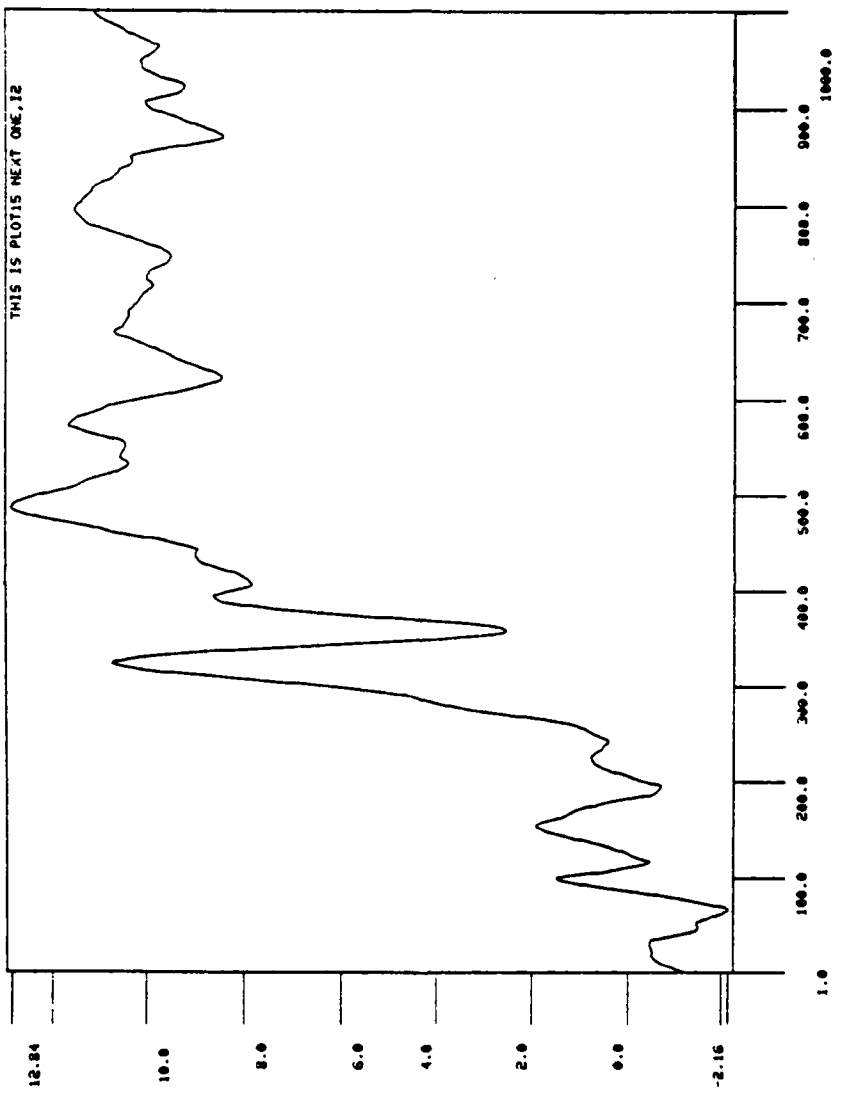

Figure 5-12. Angle Error - Dual/RTLS Controller - COSRO

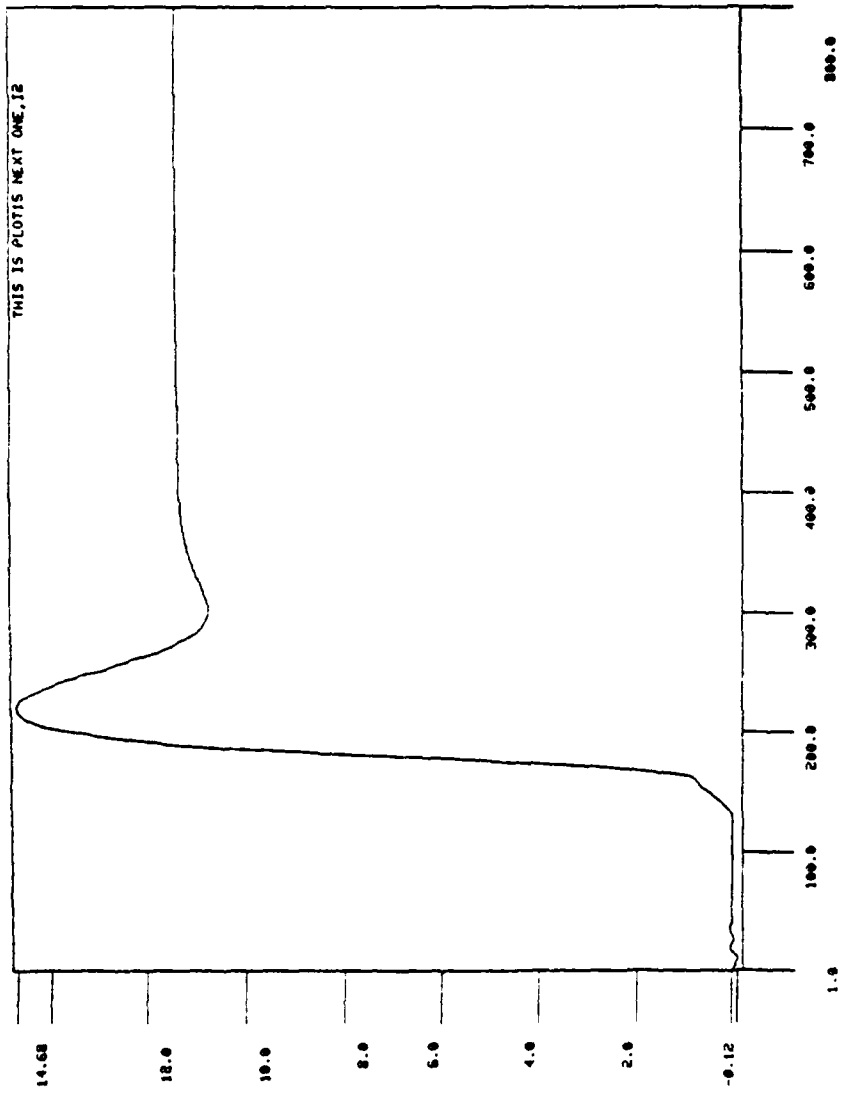

Figure 5-13. Angle Error - Open-Loop Controller - COSRO

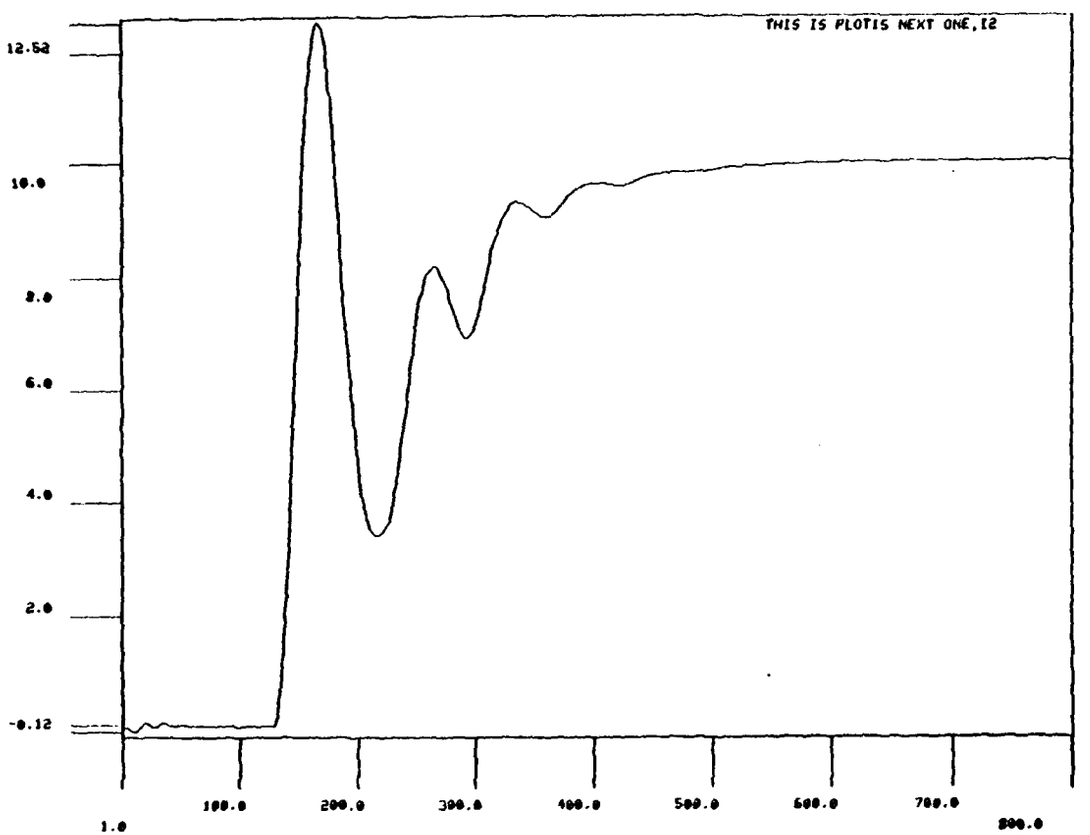

Figure 5-14. Angle Error - CE/RTLS Controller - COSRO

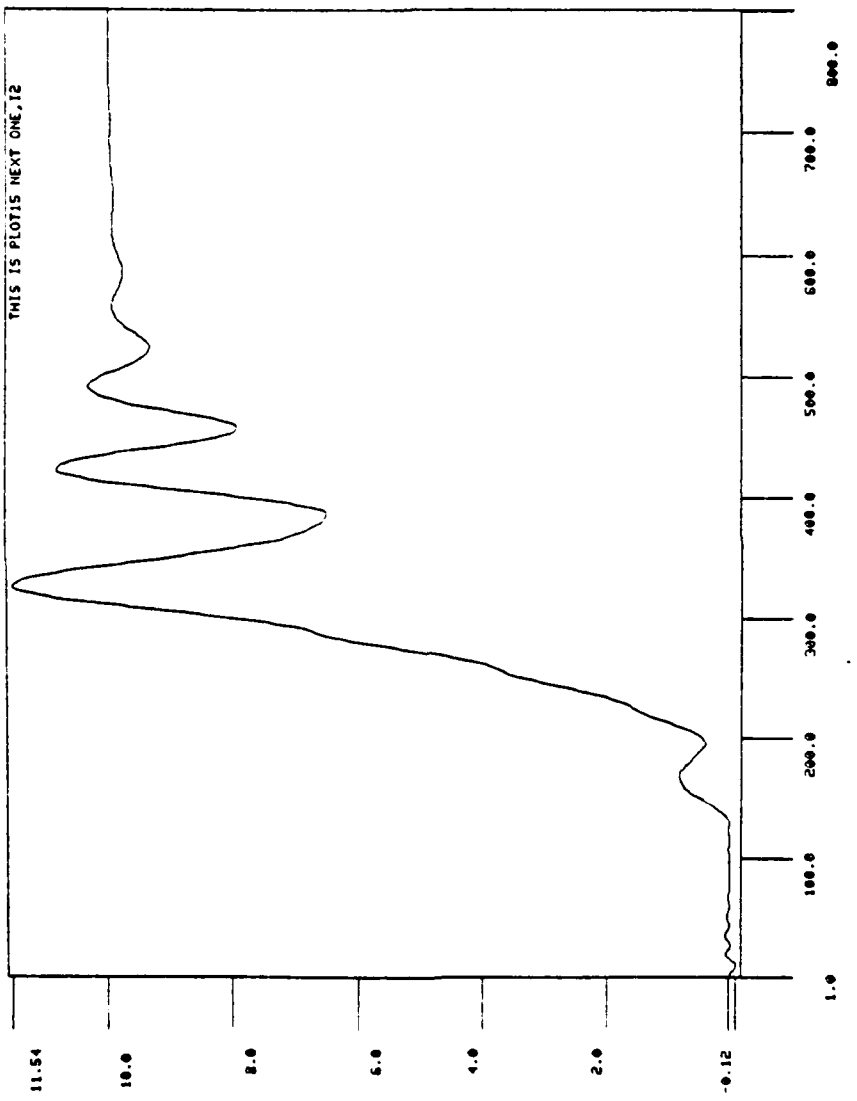

Figure 5-15. Angle Error - Cautious/RTLS Controller - COSRO

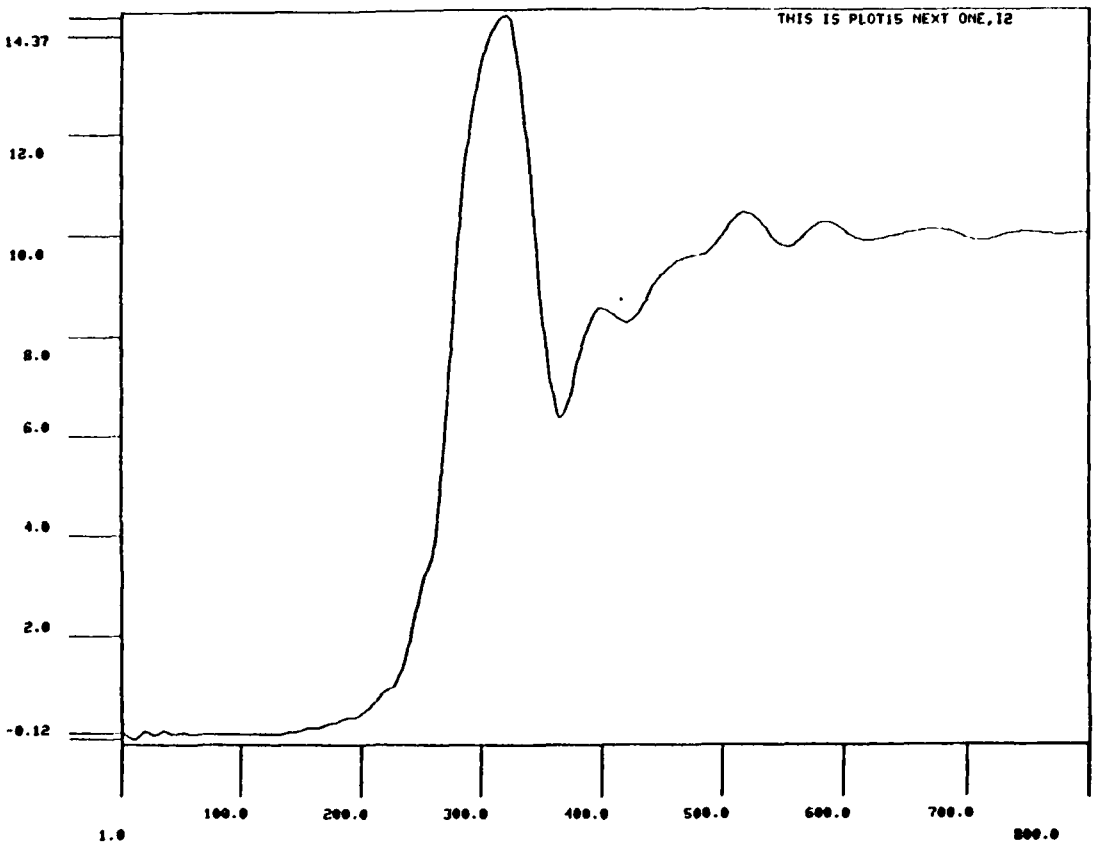

Figure 5-16. Angle Error - Dual/RTLS Controller - COSRO

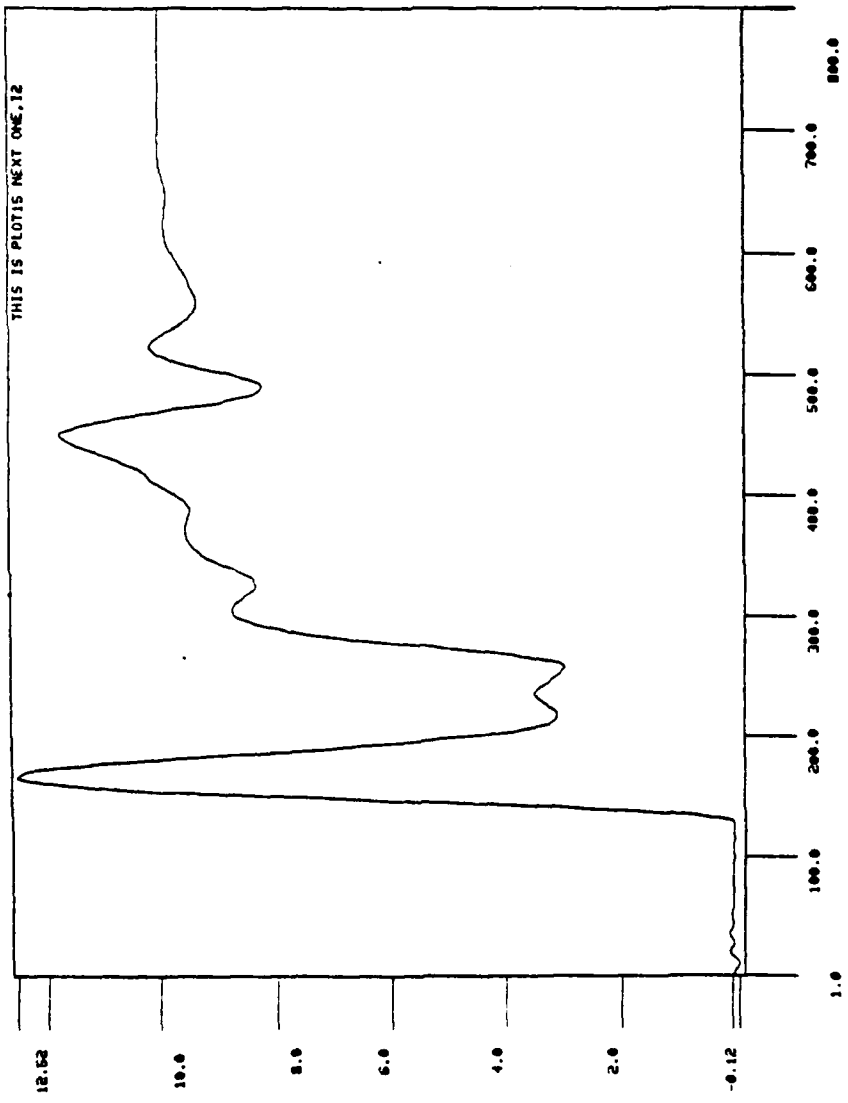

Figure 5-17. Angle Error - Cautious/RIV Controller - COSRO

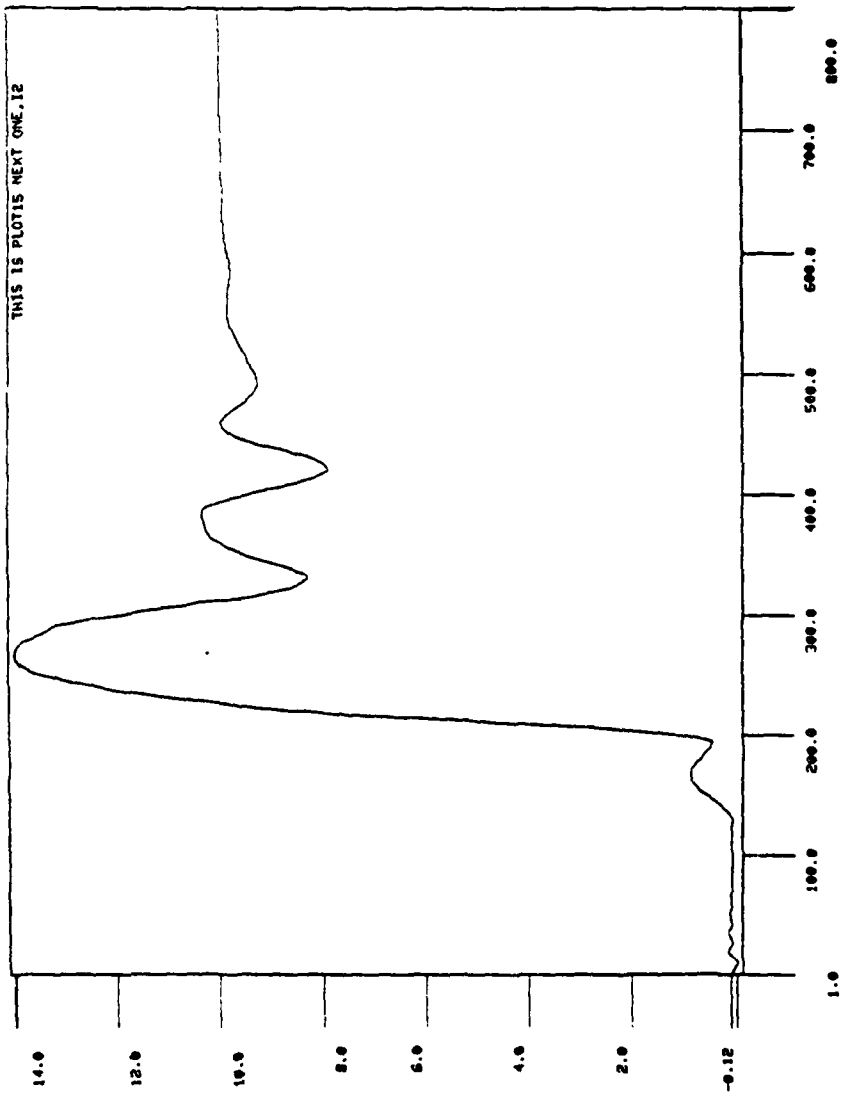

Figure 5-18. Angle Error - Dual/RIV Controller - COSRO

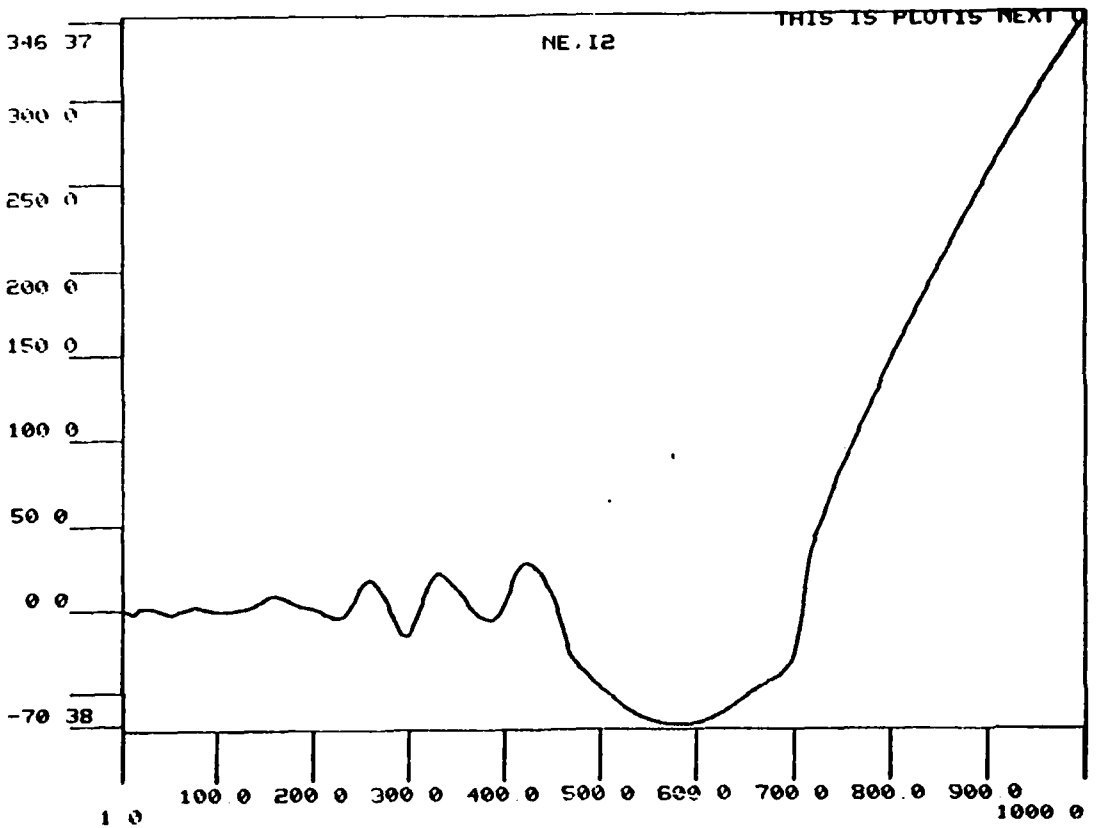

Figure 5-19. Angle Error - Cautious/RTLS Controller - COSRO

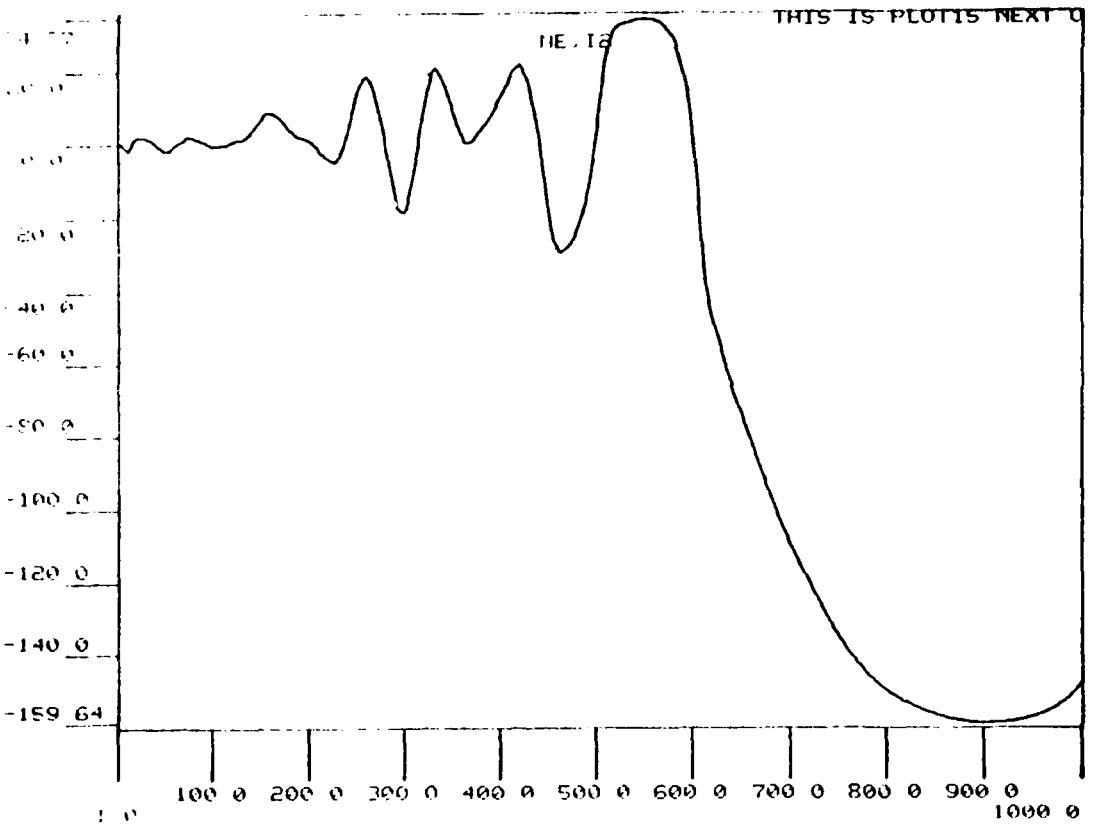

Figure 5-20. Angle Error - Cautious/RTLS Controller - COSRO

5.2 SAMPLE RUNS FOR PSUEDO-MONOPULSE

Table 5-2 describes the sample runs done against the psuedo-monopulse radar system, with Figures 5-21 through 5-26 giving outputs. The plot types are given in Section 5.1.

Figure 5-21 is the baseline result for psuedo-monopulse when no ECM is applied. Figures 5-22 through 5-26 are sample runs for the parametric controller (see Section 3.2.1); no runs are presented for the input/output controller for this radar system. The angle errors for the azimuth and elevation is given separately in Figures 5-23 and 5-24, respectively. The 90° phase shift indicates the "orbiting" behavior of the pointing angle. The error signal at the output of the summing junction (see Figure 3-2) is given in Figure 5-26 to indicate that the ECM technique does indeed introduce an error signal that is not subtracted out.

Table 5-2 Sample Runs Against Psuedo-monopulse

FIGURE	PLOT TYPE	REFERENCE ANGLE	CONTROLLER
5-21	3	0.3 BW	No ECM
5-22	1	0.3 BW	Adaptive parametric
5-23	9 (Azimuth)	0.3 BW	Adaptive parametric
5-24	9 (Elevation)	0.3 BW	Adaptive parametric
5-25	5	0.3 BW	Adaptive parametric
5-26	10	0.3 BW	Adaptive parametric

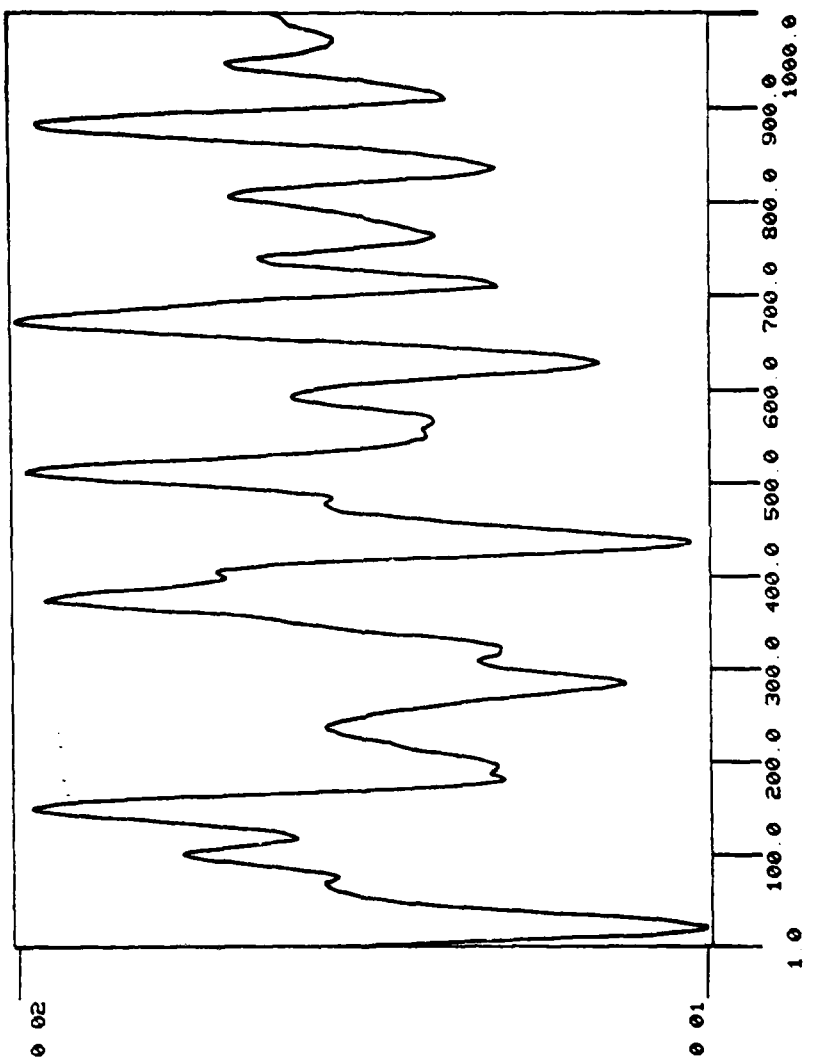

Figure 5-21. Angle Error - No ECM - Psuedo-Monopulse

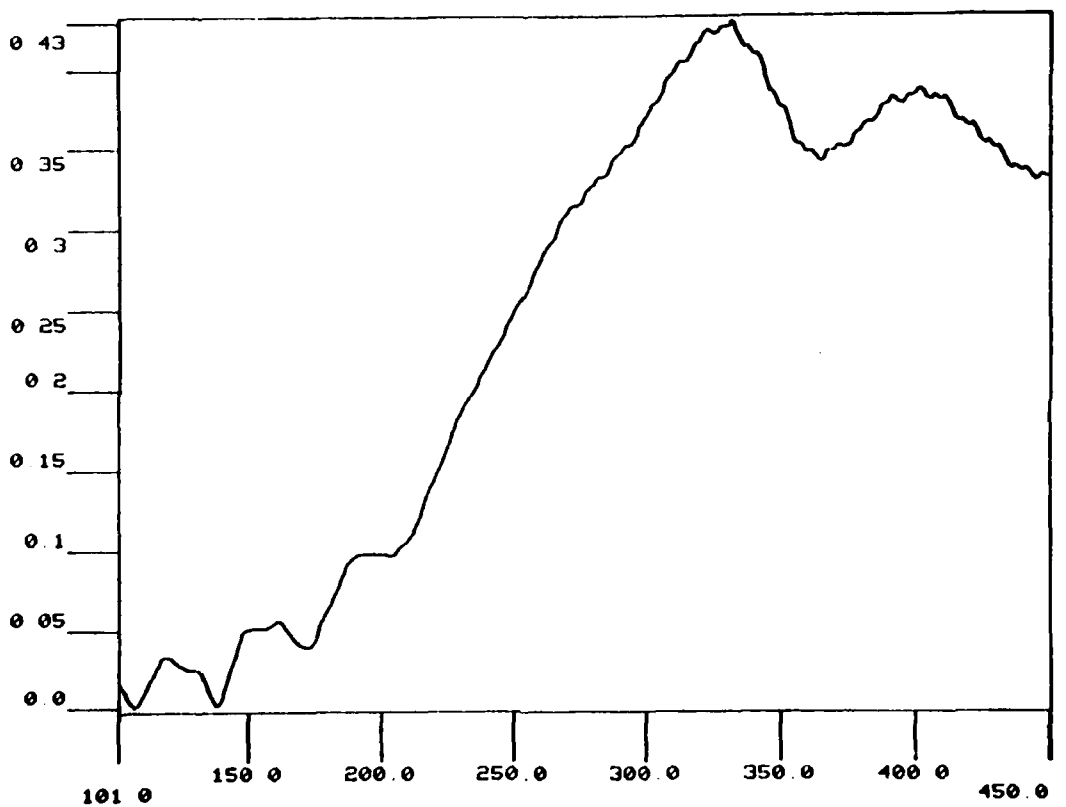

Figure 5-22. Angle Error - Adaptive Parametric Controller - Psuedo-Monopulse

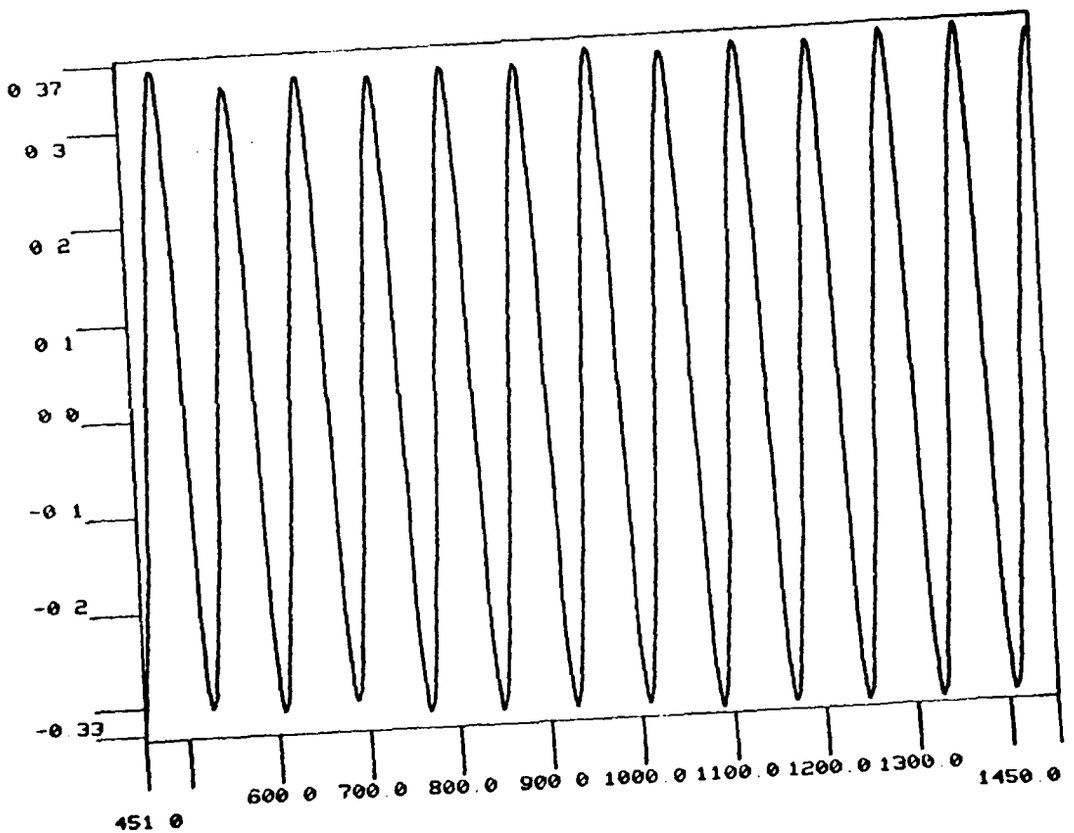

Figure 5-23. Azimuth Angle Error - Adaptive Parametric Controller - Psuedo-Monopulse

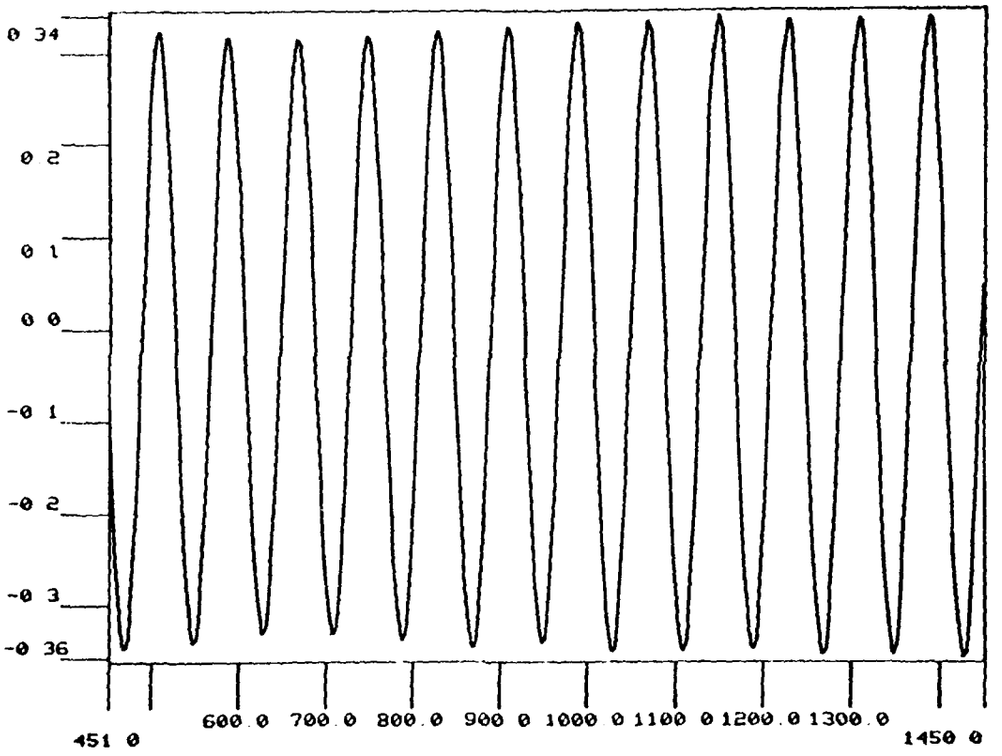

Figure 5-24. Elevation Angle Error - Adaptive Parametric Controller - Psuedo Monopulse

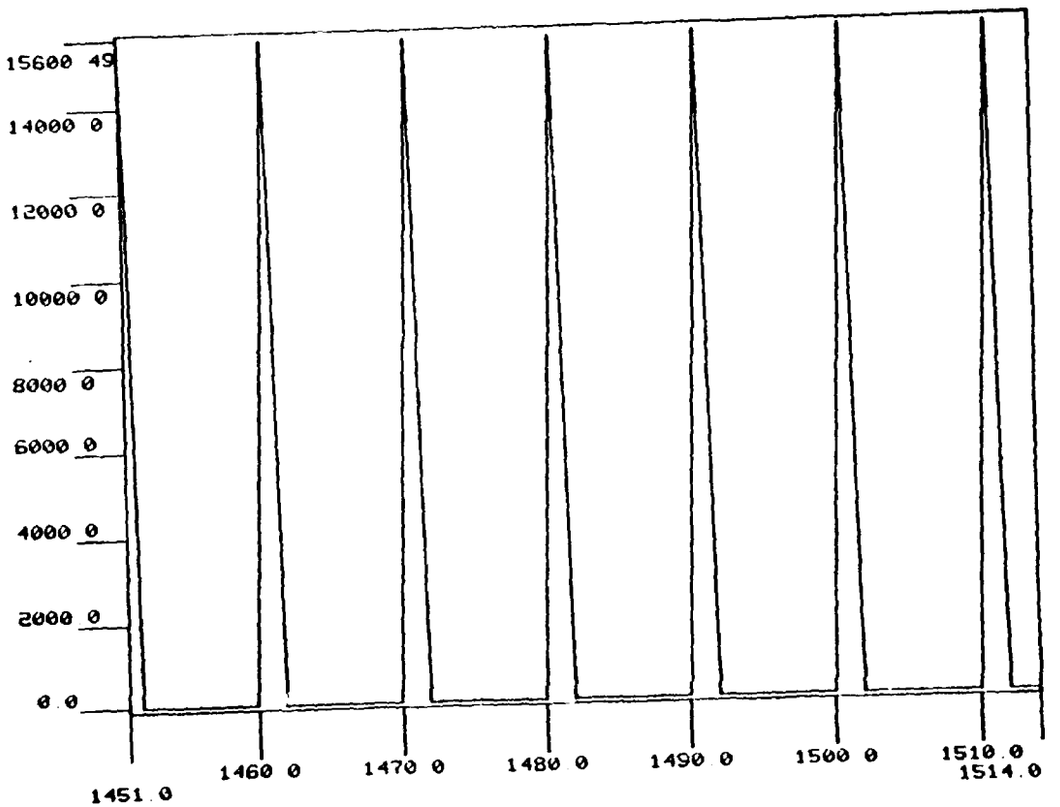

Figure 5-25. ECM Signal - Adaptive Parametric Controller - Psuedo-Monopulse

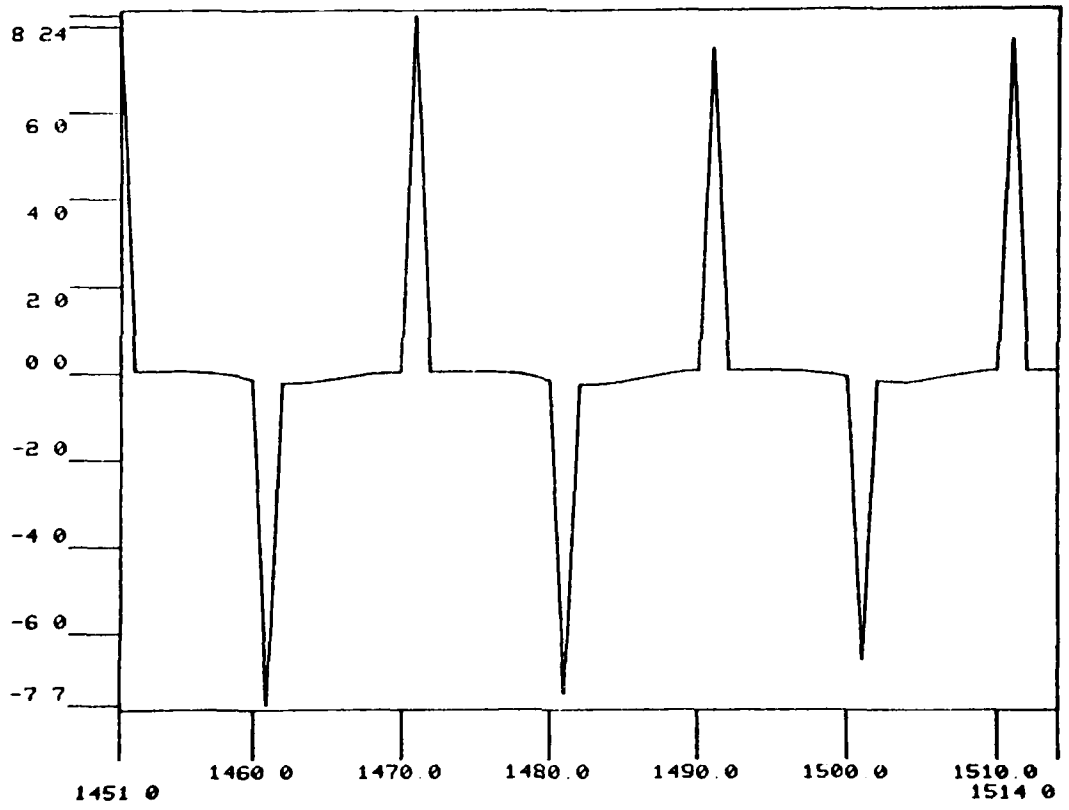

Figure 5-26. Error Signal - Adaptive Parametric Controller - Psuedo-Monopulse

5.3 SAMPLE RUNS FOR MONOPULSE

Table 5-3 describes the sample runs done against the monopulse radar system, with Figures 5-27 through 5-34 giving outputs. The plot types are given in Section 5.1.

Figures 5-27 through 5-34 are sample runs for the input/output controller (see Section 4.2); no runs are presented for the parametric controller for this radar system as the controller has not been designed. Figures 5-27 through 5-30 are using the cautious controller with RTLS. By this time it was decided that due to performance and ease of implementation, this controller is probably best in most applications. Angle errors and ECM signals are given, both in the transition region and in steady-state. A new controller, the input matching controller [1], was found to perform quite well for this system. Its outputs are given in Figures 5-31 through 5-34. This controller does not perform identification as the others do, so there is no breakdown of time into these two phases.

Table 5-3. Sample Runs Against Monpulse

FIGURE	PLOT TYPE	REFERENCE ANGLE	CONTROLLER
5-27	1	0.3 BW	Cautious with RTLS (see Note 1)
5-28	5	0.3 BW	Cautious with RTLS (see Note 1)
5-29	3	0.3 BW	Cautious with RTLS (see Note 1)
5-30	5	0.3 BW	Cautious with RTLS (see Note 1)
5-31	1	0.3 BW	Input Matching
5-32	5	0.3 BW	Input Matching
5-33	3	0.3 BW	Input Matching
5-34	5	0.3 BW	Input Matching

Note

1 - Identification only until pulse number 200.

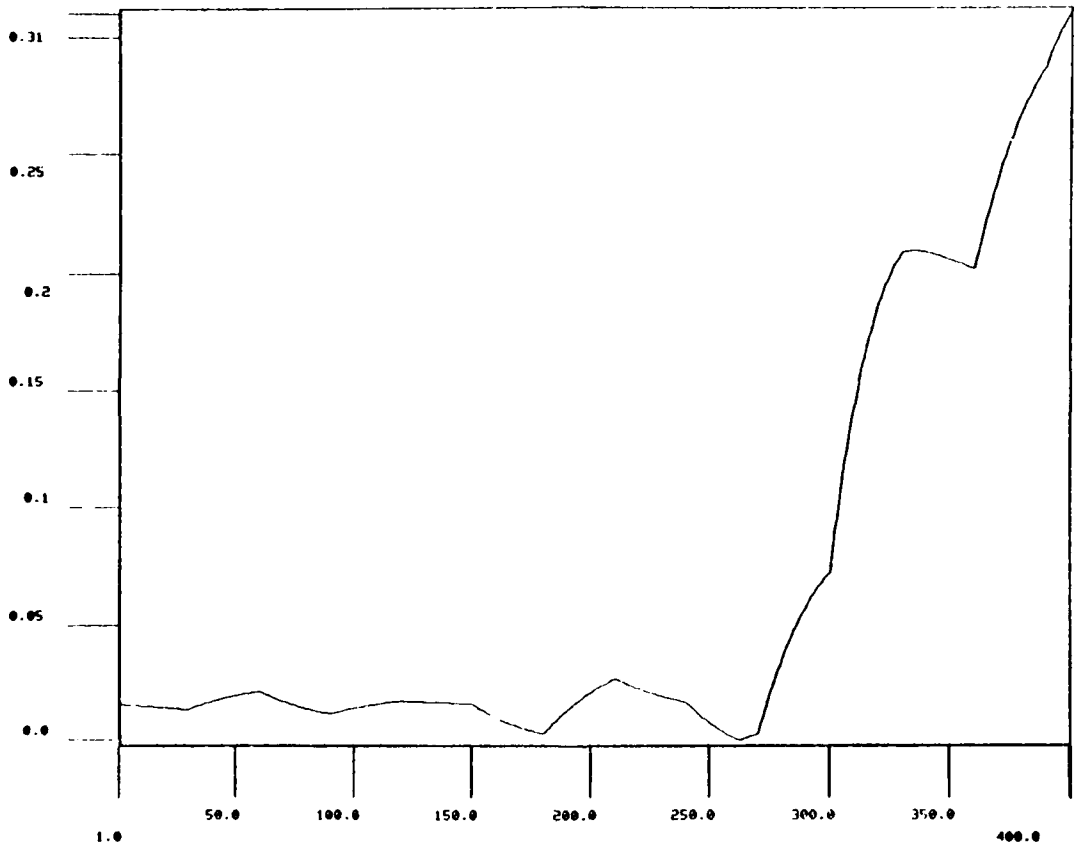

Figure 5-27. Angle Error - Cautious/RTLS Controller - Monopulse

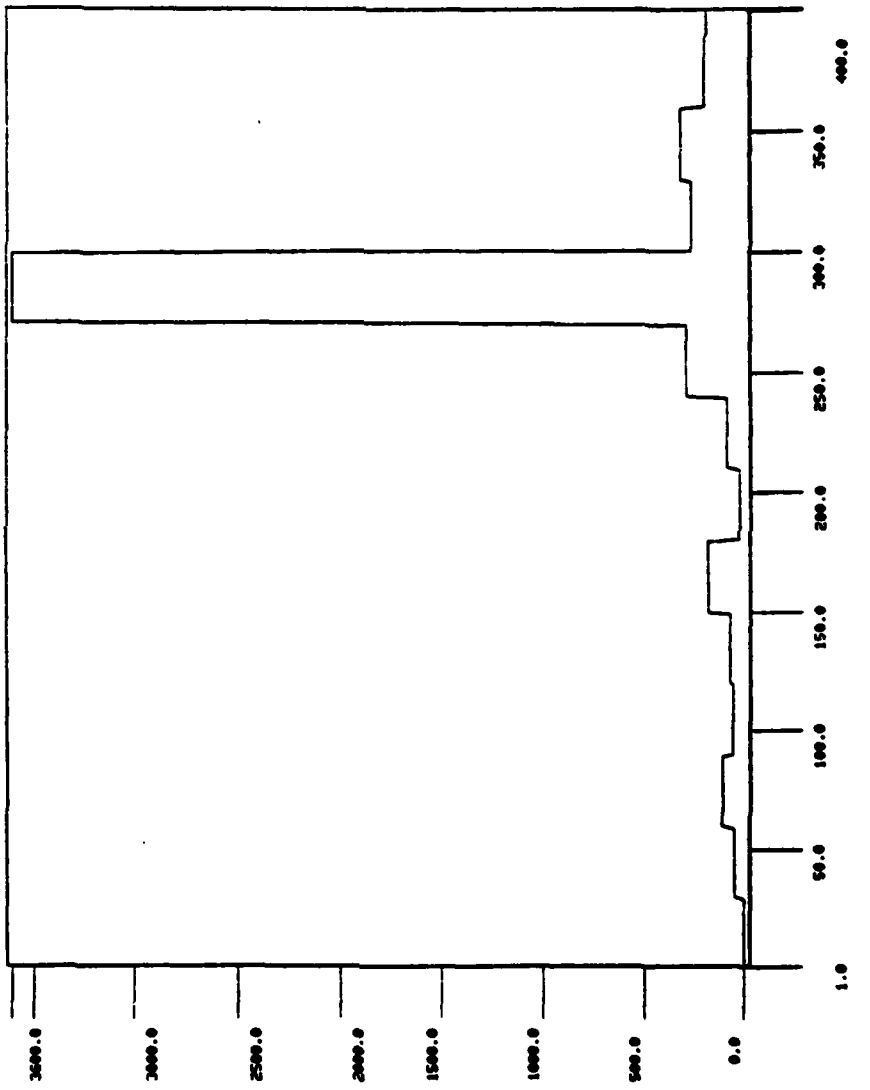

Figure 5-28. ECM Signal - Cautious/RTLS Controller - Monopulse

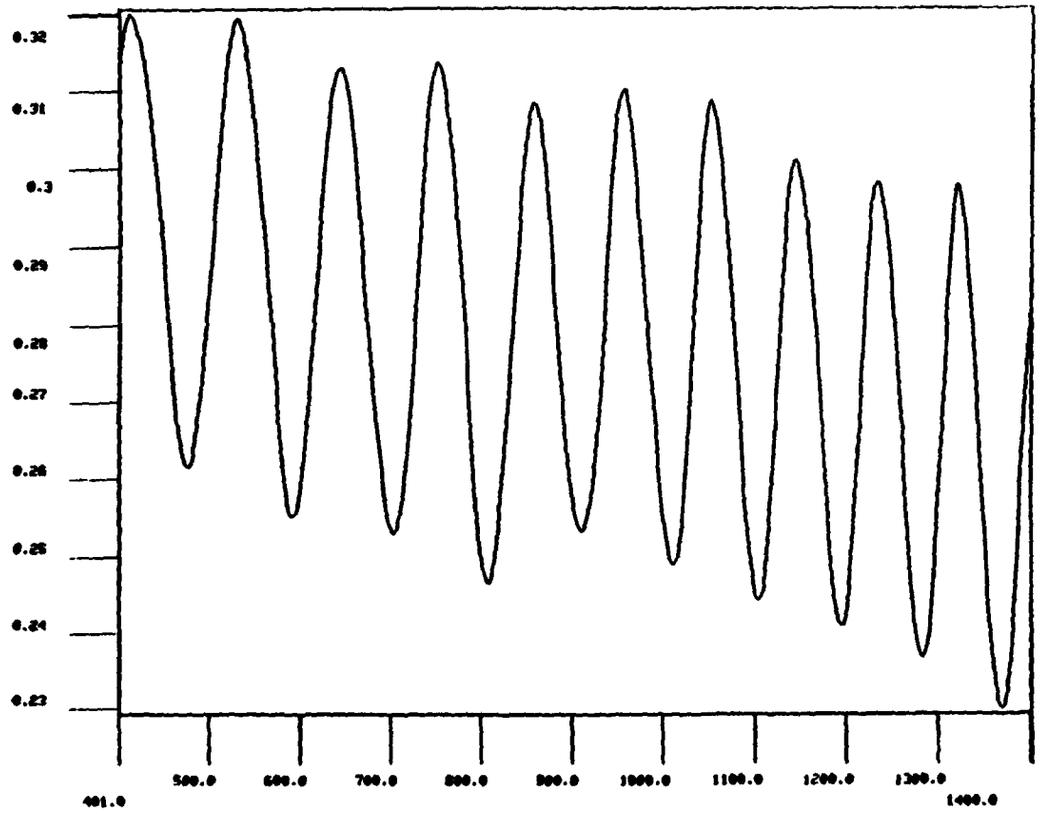

Figure 5-29. Angle Error - Cautious/RTLS Controller - Monopulse

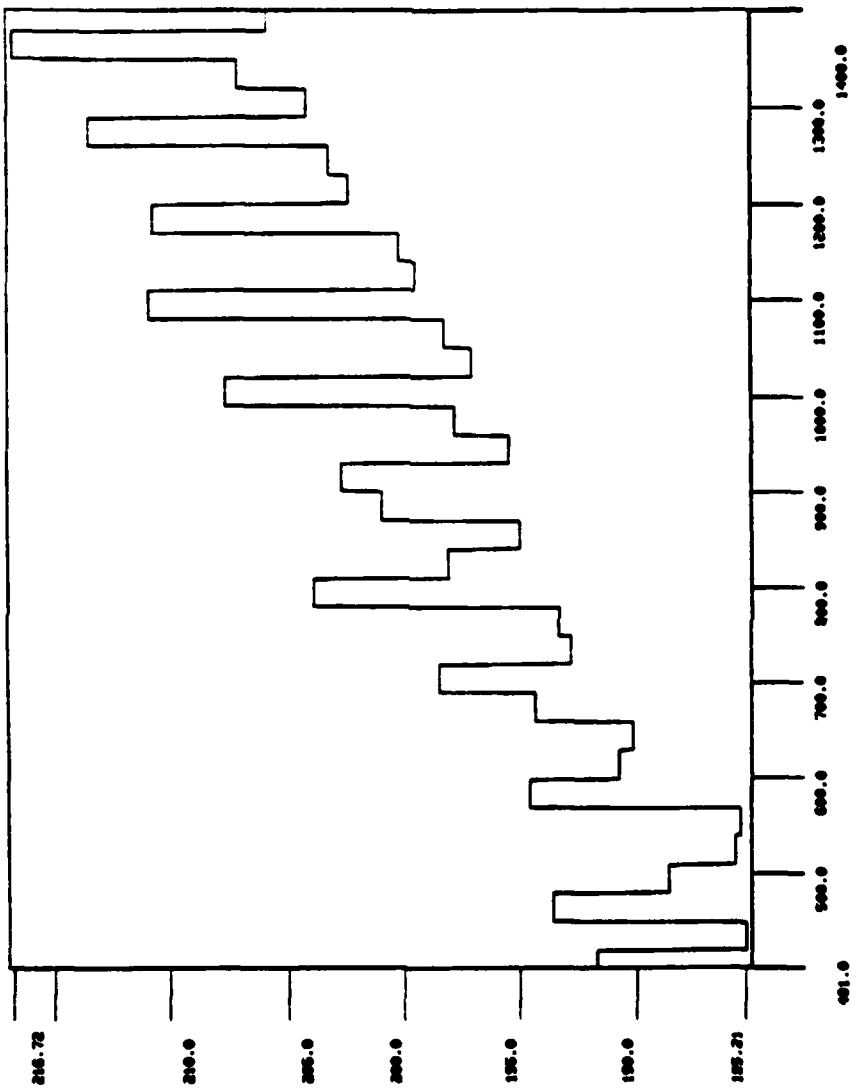

Figure 5-30. ECM Signal - Cautious/RTLS Controller - Monopulse

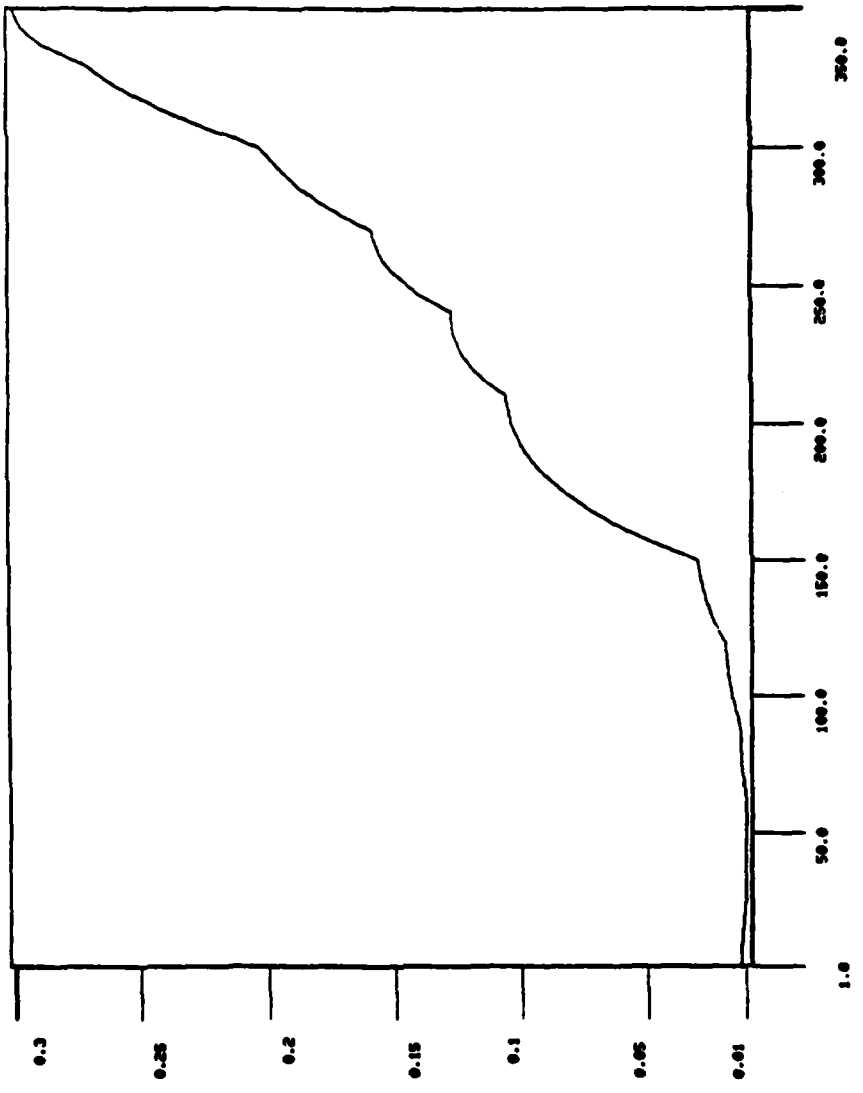

Figure 5-31. Angle Error - Input Matching Controller - Monopulse

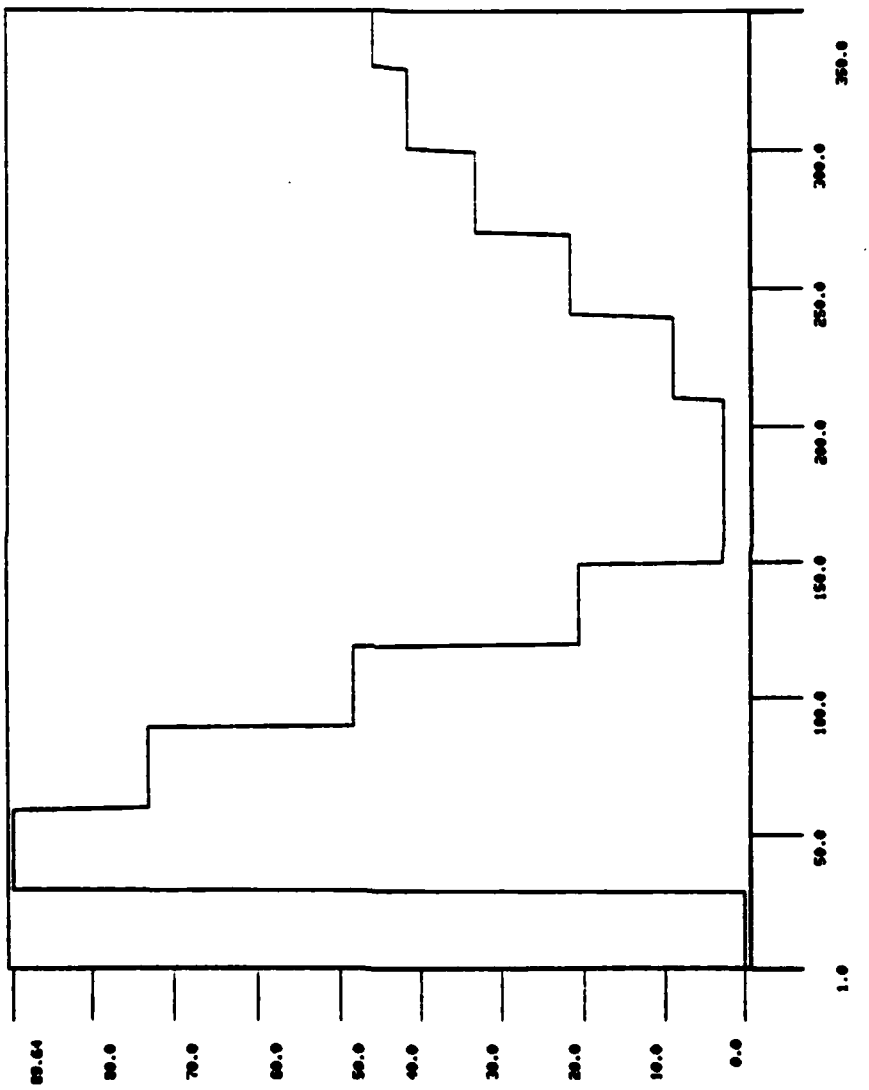

Figure 5-32. ECM Signal - Input Matching Controller - Monopulse

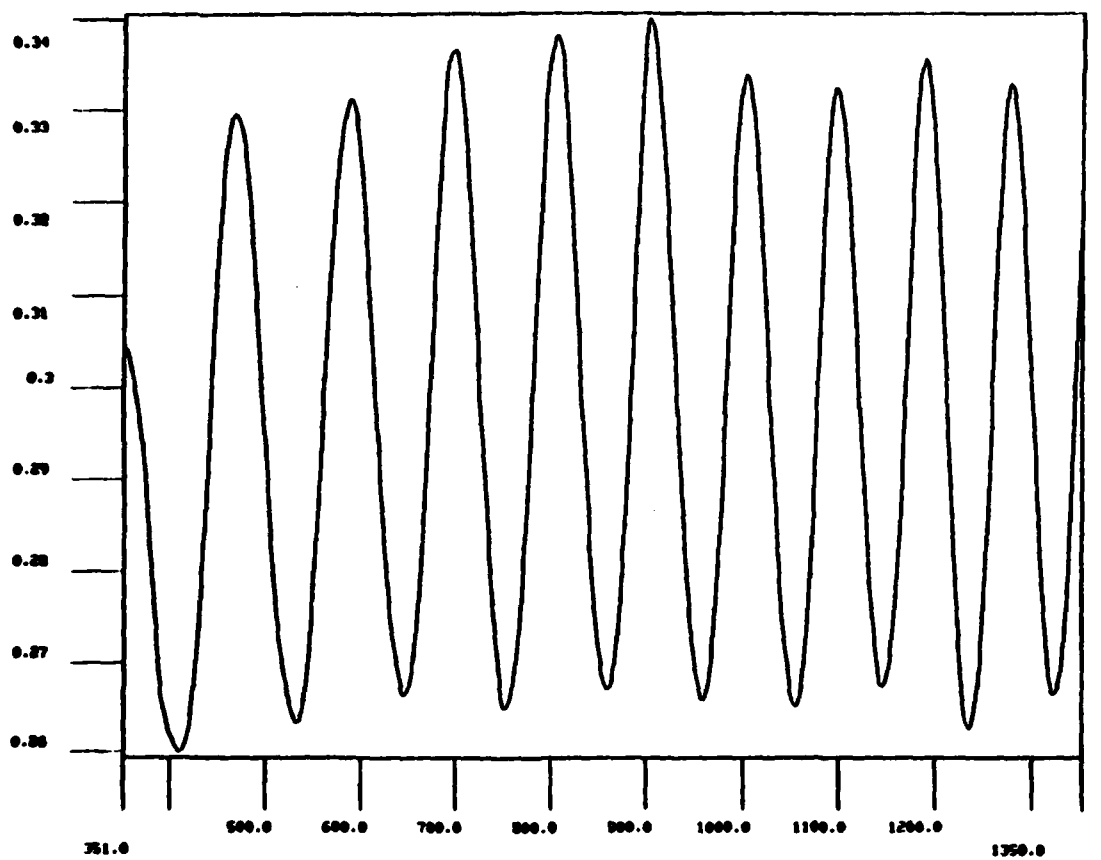

Figure 5-33. Angle Error - Input Matching Controller - Monopulse

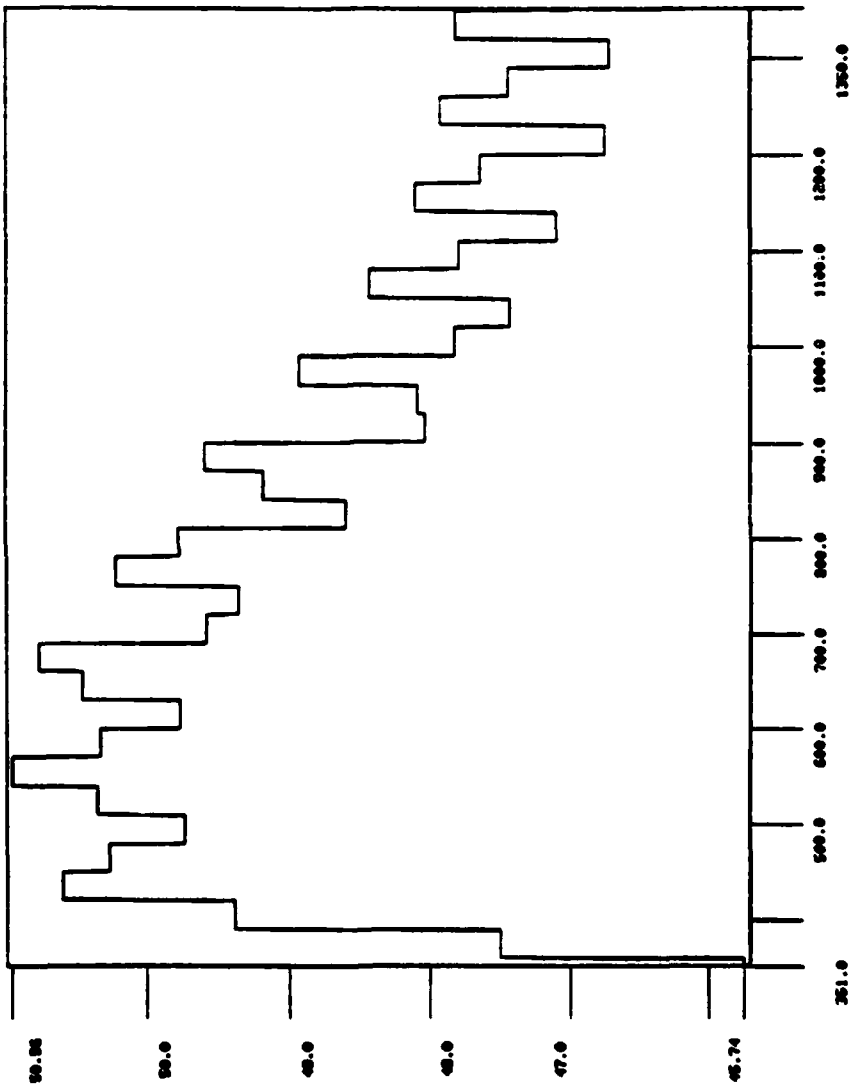

Figure 5-34. ECM Signal - Input Matching Controller - Monopulse

REFERENCES

1. A.J. Rockmore, B. Friedlander, L.R. Keearns, "Development of Adaptive Closed-Loop Control Procedures for Electronic Countermeasures," Systems Control, Inc., Project 5302, Task 1 Technical Report, August 1979.

2. P.L. Cowell, B. Friedlander, A.J. Rockmore, "Application of Adaptive Closed-Loop Control Procedures for Electronic Countermeasures (U)," Systems Control, Inc., Project 5302, Task 2 Technical Report, Report No. PA 80-187, September 1980 (SECRET).

3. A.V. Oppenheim, R.W. Schafer, Digital Signal Processing, Prentice-Hall, 1975.